Science of the Total Environment 914 (2024) 169979

Contents lists available at ScienceDirect

Science of the Total Environment

journal homepage: www.elsevier.com/locate/scitotenv

The physiological effect of polystyrene nanoplastic particles on fish and human fibroblasts

Maoxiao Peng [a,1], Rute C. Félix [a,1], Adelino V.M. Canário [a,b], Deborah M. Power [a,b,*]

[a] Centre of Marine Sciences (CCMAR/CIMAR), Campus de Gambelas, Universidade do Algarve, 8005-139 Faro, Portugal
[b] International Institution of Marine Science, Shanghai Ocean University, Shanghai, China

HIGHLIGHTS

- PS-NP uptake differs between fish (SJD.1) and human fibroblasts (BJ-5ta and HDF).
- Effects on proliferation and migration of PS-NPs depend on their concentration, size, and cell line.
- PS-NPs have cell specific metabolic effects.
- PS-NPs consistently accumulate around the nucleus and on the cell membrane system.

GRAPHICAL ABSTRACT

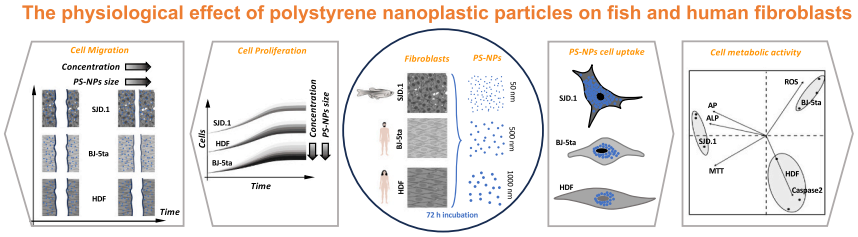

ARTICLE INFO

Editor: Damià Barceló

Keywords:
Environmental pollution
Polystyrene nanoplastics
Fibroblasts
Nanoplastics uptake
Cell migration
Cytotoxic activity

ABSTRACT

Numerous studies have identified the detrimental effects for the biosphere of large plastic debris, the effect of microplastics (MPs) and nanoplastics (NPs) is less clear. The skin is the first point of contact with NPs, and skin fibroblasts have a vital role in maintaining skin structure and function. Here, a comparative approach is taken using three fibroblast cell lines from the zebrafish (SJD.1), human male newborn (BJ-5ta) and female adult (HDF/TERT164) and their response to polystyrene NP (PS-NPs) exposure is characterized. Cells were exposed to environmentally relevant PS-NP sizes (50, 500 and 1000 nm) and concentrations (0.001 to 10 μg/ml) and their uptake (1000 nm), and effect on cell viability, proliferation, migration, reactive oxygen species (ROS) production, apoptosis, alkaline phosphatase (ALP) and acid phosphatase (AP) determined. All fibroblasts took up PS-NPs, and a relationship between PS-NP particle size and concentration and the inhibition of proliferation and cell migration was identified. The inhibitory effect of PS-NPs on proliferation was more pronounced for human skin fibroblasts. The presence of PS-NPs negatively affected fibroblast migration in a time-, size- and concentration-dependent manner with larger PS-NPs at higher concentrations causing a more significant inhibition of cell migration, with human fibroblasts being the most affected. No major changes were detected in ROS production or apoptosis in NP challenged fibroblasts. While the ALP activity was increased in all fibroblast cell lines, only fish fibroblasts showed a significant increase in AP activity. The heterogeneous response of fibroblasts induced by PS-NPs was clearly revealed by the segregation of HDF, BJ.5ta and SJD.1 fibroblasts in principal component analysis. Our results demonstrate that PS-NP exposure adversely affected cellular processes in a cell-type and dose-specific manner in distinct fibroblast cell lines, emphasizing the need for further exploration of NP interactions with different cell types to better understand potential implications for human health.

* Corresponding author at: Centre of Marine Sciences, Campus de Gambelas, Universidade do Algarve, 8005-139 Faro, Portugal.
E-mail address: dpower@ualg.pt (D.M. Power).
[1] These authors contributed equally to the work.

https://doi.org/10.1016/j.scitotenv.2024.169979
Received 12 August 2023; Received in revised form 3 January 2024; Accepted 5 January 2024
Available online 10 January 2024

1. Introduction

Global plastic production is correlated to the impact of environmental pollution caused by plastics. In 2021, worldwide production reached approximately 391 million tones and has been growing by an average of 9 % per year (Plastics Europe, 2022). Although large plastic fragments can cause harm to animals, the fragmentation of larger pieces into microplastics (MPs, particle diameter < 5 mm) and nanoplastics (NPs, particle diameter < 1 μm), poses a more significant threat to living organisms (Sana et al., 2020; Wang et al., 2021). Furthermore, the production of MP and NP materials for industrial applications are inevitably adding to the burden of plastics in the environment (Desidery and Lanotte, 2022; Hu et al., 2022; Kumar et al., 2021; Walker and Fequet, 2023). Smaller plastic fragments disperse easily in the environment, which makes their removal challenging (Andrady, 2011; Cózar et al., 2014; Ter Halle et al., 2017) and facilitates their penetration into cells and organs (Lehner et al., 2019).

MPs and NPs are widespread and they can be found in aquatic systems (oceans, rivers, and lakes), soil, and even the atmosphere (Boucher et al., 2019; Chen et al., 2021; Cózar et al., 2017; Zhang et al., 2016). They are ubiquitous in the environment and exist in widely varying concentrations (*e.g.* 0.001 μg/ml to 0.01 μg/ml in water samples and 1.6 μg/ml in human blood) (Chang et al., 2022; Eerkes-Medrano et al., 2015; Jambeck et al., 2015; Lenz et al., 2016; Leslie et al., 2022; Li et al., 2022; Zhou et al., 2021, 2019), and although they are readily taken up by organisms their toxicity is still unclear (Lehner et al., 2019). The pervasiveness and persistence of MPs and NPs in the environment, is reflected by their presence in drinking water and bottled water (Schymanski et al., 2018), and has raised significant concern due to their negative consequences for human health (Lehner et al., 2019; Rubio et al., 2020b; Sana et al., 2020). To date, > 70 % of NP/MP-related research is focused on MPs, and approximately 90 % of NP research is focused on polystyrene (PS), one of the most produced plastics globally and a major part of plastic litter in the oceans, as well as in surface water (Barboza et al., 2020; Pelegrini et al., 2023). The size of plastic particles directly influences their toxicity and particles at the nanometer scale are more toxic than those of the micrometer scale due to their stronger penetrating and absorbing properties (Bobori et al., 2022; Jeong et al., 2016). For example, meta-analysis of the effects of plastics of the same material (polystyrene) on 20 physiological indexes in a diversity of species revealed that the toxicity of NPs was greater than MPs, especially in the index survival/lethality (Pelegrini et al., 2023).

NPs can enter organisms through various routes, including ingestion (directly or *via* the food chain), inhalation, and dermal contact and have been found in plant roots, zooplankton, shellfish, in a diversity of fish and human tissues, and even human feces (Barría et al., 2020; Bobori et al., 2022; del Real et al., 2022; Jiang et al., 2020; Lehner et al., 2019; Li et al., 2020; Lins et al., 2022). The cellular uptake of particles begins by adhesion to the cell membrane followed by uptake by passive penetration or active endocytosis (Fiorentino et al., 2015; Lesniak et al., 2013; Wang et al., 2012). The endocytic pathway depends on particle size and cell type and the mechanism is only partially understood (Liu et al., 2021).

Most of the screening for MP/NP toxicity is based on whole animal exposure and is biased towards marine organisms due to the well documented and alarming levels of contamination in the marine biosphere (Cózar et al., 2014; Guzzetti et al., 2018; Peng et al., 2020; Thushari and Senevirathna, 2020). Studies focused on the adverse effects of MP/NP toxicity in soil systems have explored their potential interactions with contaminants, including pesticides and heavy metals, their transfer through the food chain and potential harmful effects (de Souza Machado et al., 2018; Dissanayake et al., 2022; Mendes, 2022). Ethical concerns about the use of animals to assess MP/NP toxicity and the cost, time and unpredictability of such studies has increased pressure to find alternatives to animal testing. For this reason, development of reliable and rapid *in vitro* screening approaches, not dependent on animals, is a priority. Such *in vitro* approaches and the data they generate complement data about the chemical composition and concentration of nano-sized materials in the environment and are essential for risk assessment of their likely biological and ecosystem wide effects.

Existing *in vitro* studies have demonstrated the importance of MP and NP size and surface charge on cellular toxicity and uptake by immortal human cells (Banerjee et al., 2021; He et al., 2020; Rubio et al., 2020a). A range of immortalized cell lines or primary cultures (*e.g.*, fibroblasts, monocytes, hepatocytes, lung cells, gastric cells and leukocytes) have revealed that MP/NP exposure elicits varying effects including, but not only, reduced cell viability, an inflammatory response, increased ROS production, genotoxicity and DNA damage, micronuclei and effects on mitochondria (Banerjee et al., 2021; Gautam et al., 2022; He et al., 2020; Li et al., 2023; Lin et al., 2022; Poma et al., 2019; Rubio et al., 2020a; Shi et al., 2021). The response to MPs/NPs of fibroblasts, one of the most abundant cell types in the skin dermis (Braff and Gallo, 2006; Eming et al., 2014; Khan et al., 2018), is poorly studied but NPs larger than 100 nm are not thought to penetrate the stratum corneum of skin (Bouwstra et al., 2001), although entry through hair follicles, sweat glands (Schneider et al., 2009) and damaged skin readily occurs (Jatana et al., 2016; Mortensen et al., 2008). Furthermore, the use of transdermal drug delivery systems using NPs indicates an unexpected skin permeability particularly when chemical enhancers are used (Krishnan and Mitragotri, 2020; Zeng et al., 2023). Given the ubiquitous nature of NPs in the environment and the constant exposure of skin to them in both terrestrial and aquatic organisms a better understanding of how NPs affect skin cells is urgent particularly in the highly biodiverse non-mammalian aquatic vertebrates (>28,000 extant teleost fish exist) (Volff, 2005).

In this study several fibroblast cell lines from human and fish skin that differ in physiology, barrier function and regenerative properties were used (Abe et al., 2020; Niethammer et al., 2009; Rakers et al., 2010; Richardson et al., 2013 to investigate the effects of nanoparticles. Fibroblasts were from adult zebrafish (SJD.1) skin, which is a mucosal barrier and human newborn male (BJ-5ta) and adult female (HDF) skin, which is a cornified barrier. While previous *in vitro* studies have predominantly focused on the effects of high NP concentrations (Carballo et al., 2018; Lihua and Zhiyin, 2023), the potential consequences of lower concentrations, akin to those encountered in the environment (0.001 μg/ml to 0.01 μg/ml in water samples) or in humans (up to 1.6 μg/ml in human blood) remain underexplored (Lenz et al., 2016; Leslie et al., 2022; Li et al., 2022; Zhou et al., 2021, 2019). The consequence of PS-NP exposure on the physiology of skin fibroblast cell lines of different origin, sex and developmental age was established using an *in vitro* screening approach. Comparative research on the absorption capacity, physiological response and behaviour of different cell lines exposed to PS-NPs will contribute essential data for knowledge based risk assessment of their likely effects on fish and human health.

2. Material and methods

An overview of the experiments and NP size and concentrations used in each assay of the present study and reported in the respective section of the methods can be found in Fig. 1. This study included environmentally relevant PS-NP sizes (50, 500 and 1000 nm) and concentrations (0.001 μg/ml to 10 μg/ml). Specific attention was given to the concentration of 1 μg/ml since it is proximate to concentrations found in some human blood samples (up to 1.6 μg/ml) (Leslie et al., 2022). Preliminary experiments were conducted using PS-NPs labelled with a green fluorescent protein (GFP), as they facilitate imaging and confirmation of cell uptake with smaller sized NPs. However, comparative assays using 1 μm GFP-labelled PS-NPs and plain PS-NPs revealed the fluorescent label altered the behavior and uptake of PS-NPs as has previously been reported (Jeon et al., 2018). For this reason plain PS-NPs were used in all assays to ensure consistency and to mitigate potential artifacts arising from fluorescent PS-NPs.

Plain polystyrene Nanoplastics (PS-NPs) were obtained from

Phosphorex, Polystyrene Nanoparticles (USA) in aqueous suspension (1 % solids). All nanoparticles purchased had a polystyrene density of 1.06 g/ml^3 and before use the stock solutions were sonicated and thoroughly vortexed. The molecular structure of PS-NPs was confirmed with Fourier-transform infrared spectroscopy (FTIR). The FTIR spectra was recorded with Infrared Microscopy (μ-FTIR) - Nicolet iN10MX (Thermo Fisher Scientific) with a detector MCT/A in mode ATR-15 (32 scans with 4 cm^{-1} resolution) and this confirmed the molecular structure of all PS-NPs used in this study (Supplementary Fig. 1). To avoid interference in the assays of free PS-NPs in the culture medium the cells were pre-incubated for 72 h with the PS-NPs and washed before use to remove free particles.

2.1. Culture of fibroblast cells

2.1.1. Human cell lines

The cell line BJ-5ta (ATCC® CRL-4001™) used in the study was isolated from hTERT-immortalized fibroblasts from human male foreskin (*Homo sapiens*). The cryopreserved cells were defrosted and then cultures initiated following the supplier's instructions. The culture medium used for BJ-5ta was composed of a 4:1 mixture of DMEM:M199 supplemented with Fetal bovine serum (FBS) (10 %), Hygromycin B (1 %) and Ampicillin (1 %). Cultures were maintained in a humid 5 % CO_2 incubator (Heraeus, Hanau, Germany) at 37 °C. The cell line, HDF/TERT164 (EVERCYTE CHT-008-0164) used in the study was isolated from female skin (*H. sapiens*). The cryopreserved cells were defrosted and then cultures were initiated following the supplier's instructions. The culture medium was composed of a 1:1 mixture of DMEM: Ham's F12 supplemented with FBS (10 %), GlutaMAX (2 mM) and G418 (0.1 mg/ml). Cultures were maintained in a humid 5 % CO_2 incubator (Heraeus, Hanau, Germany) at 37 °C.

2.1.2. Fish cell line

The primary cell line SJD.1 (ATCC® CRL-2296™) used in the study is a fibroblast cell line derived from amputated caudal fins of an adult zebrafish (*Danio rerio*), a highly used fish model. The cryopreserved cells were defrosted and then cultures were initiated according to the supplier's instructions. The culture medium was composed of DMEM medium supplemented with FBS (15 %). Cultures were maintained in a humid 5 % CO_2 incubator (Heraeus, Hanau, Germany) at 28 °C.

All assays were conducted using the cell line appropriate complete medium described above. Previous optimization experiments revealed that the fibroblast cell lines used in this study, when maintained in low concentrations of FBS, exhibited a stress response that could mask or modify the cells response to PS-NPs. Thus, to ensure methodological consistency, standard concentrations of FBS (10 %) were used in all experiments.

2.2. NP uptake assay

To ensure that the NPs used in the experiment entered the cells, a cell uptake experiment was conducted with 1000 nm unlabeled PS-NPs, since these particles are readily observed by brightfield microscopy. To establish the uptake characteristics of PS-NPs the BJ-5ta, HDF, and

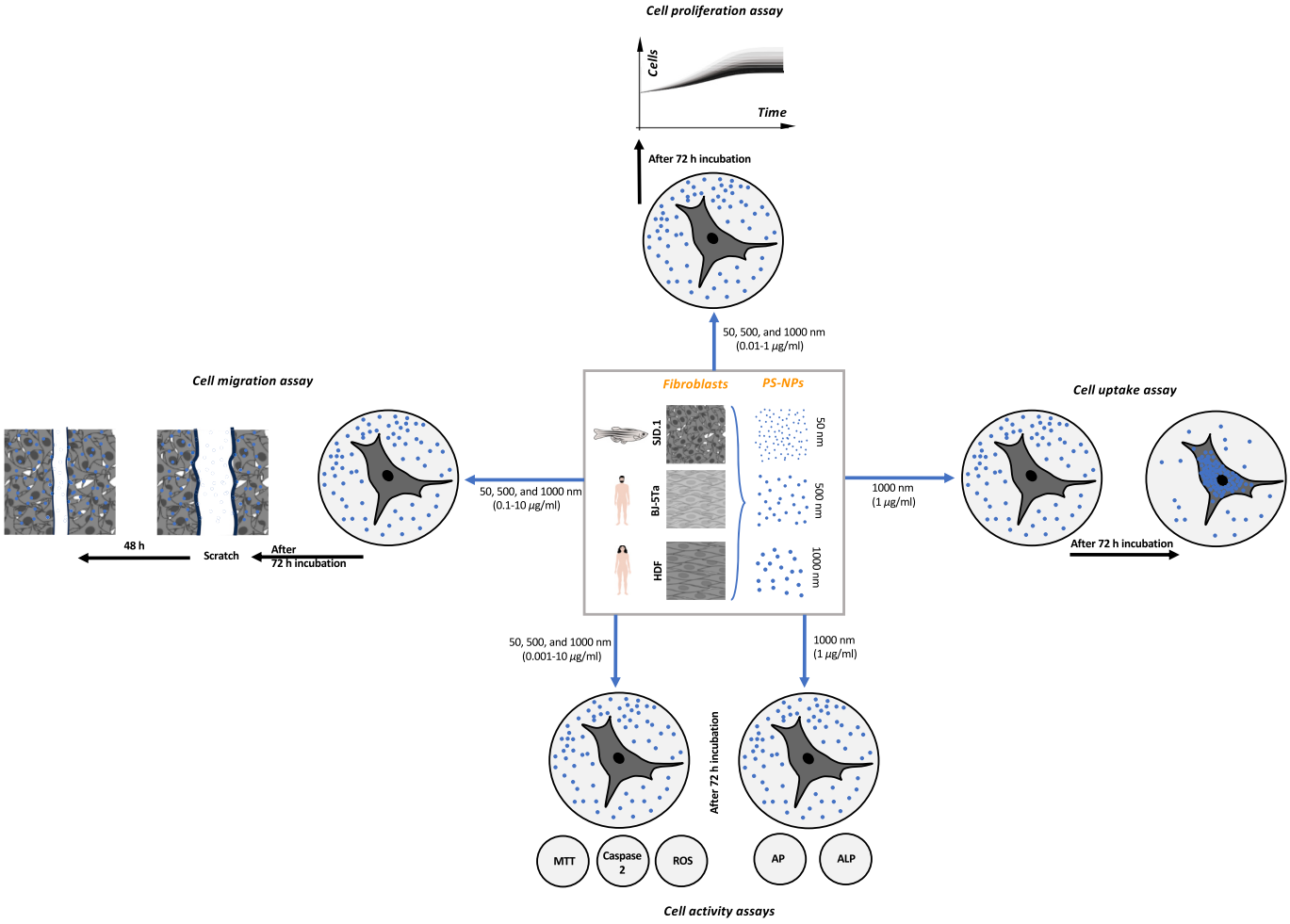

Fig. 1. Schematic of the experimental design. Four experiments were run with the 3 fibroblast cell lines (BJ-5ta, HDF and SJD.1) analyzed in the study. Cells were co-incubated with PS-NPs for 72 h before the start of the assay, and then the medium containing PS-NPs removed and the cells washed before analysis or photography.

SJD.1 fibroblasts cells from passage 2–3 were used. Cells were seeded into 24-well tissue culture plates (25,000 cells/well) and incubated overnight under optimal conditions until the cells completely adhered to the plates. After an overnight incubation of the cells, the medium was replaced with the cell-specific medium (indicated in Section 2.1) supplemented with PS-NPs (1000 nm, 1 μg/ml) (Phosphorex, Polystyrene Nanoparticles, USA), and for the control cells normal medium without PS-NPs was used; cells were then incubated for 72 h. Each experimental group was set up with six technical replicates and experiments were repeated in two independent experiments. Before imaging the medium was removed, the cells washed and new medium without PS-NPs added. Cell images were captured using a Leica DM IL microscope coupled to a Visicam PRO 20C digital camera. The number of PS-NPs inside cells was determined using ImageJ software.

2.3. Cell viability assay

Cell viability was determined using a MTT (3-(4,5-dimethylthiazol-2-yl)-2,5-diphenyltetrazolium bromide) assay, which is a colorimetric method for evaluating cellular metabolic activity. Briefly, BJ-5ta, HDF and SJD.1 cells were seeded into 96-well tissue culture plates (50,000 cells/well) and allowed to adhere overnight. After incubation, the complete medium was replaced by medium with PS-NPs of different sizes (50, 500 and 1000 nm) and concentrations (0.001, 0.01, 0.1, 1 and 10 μg/ml), and cells were incubated for 72 h under optimal conditions. A positive control (cells incubated in medium without PS-NPs) and a negative control (medium alone with no cells), for each cell line, was included in the assays. The assays were performed with six technical replicates per treatment and carried out in two independent experiments.

The MTT assay was performed following the manufacturer's instructions, and cell absorbance was measured at 540 nm using a multiplate reader (TECAN Infinite M200 Plate Reader, Switzerland). Cell viability was calculated as follows:

$$\text{Viability}\% = 100 \times (\text{ODt} - \text{ODnc})/(\text{ODc} - \text{ODnc})$$

where ODt represents the mean value of the measured optical density of the test item; ODc represents the mean value of the measured optical density of the control (cells without NPs), and ODnc represents the mean value of the measured optical density of the negative control (medium alone).

2.4. Cell proliferation assay

To establish the proliferation characteristics of the BJ-5ta, HDF and SJD.1 fibroblasts, a confluent monolayer of each type of fibroblast was dissociated from a 5 ml culture flask (Sarstedt, Nümbrecht, Germany) using Tryple™ Select digestion (Gibco, Thermo Fisher Scientific, Waltham, USA) and seeded into 24-well cell culture plates (25,000 cells/well) in the appropriate cell specific medium. After overnight incubation to permit cell adhesion the medium was replaced with the cell specific medium supplemented with PS-NPs, and the cells were incubated under optimal conditions for 72 h to allow PS-NP uptake. In the PS-NP exposed cell lines three different sizes of PS-NPs 50, 500 and 1000 nm and three concentrations, 0.01, 0.1 and 1 μg/ml were used. In the control group of each cell line medium without PS-NPs was used.

After incubation of cells with the PS-NPs, the cells were trypsinized, washed to remove NPs and seeded in the cell-specific medium into 96-well cell culture plates (5000 cells/well) prepared in quadruplicate. After cell adhesion (0 h) proliferation was followed at 48 h intervals over 168 h. Cells were counted by staining the nuclei with 40,6-diamidine-20-phenylindole dihydrochloride (DAPI, 300 nM) (Acros Organics, Waltham, MA, USA) after cell fixation with 100 % alcohol. Stained nuclei were captured in black and white digital images using a Leica DM IL microscope coupled to a Visicam PRO 20C digital camera. Images were analyzed using ImageJ software for cell counting. Proliferation curves of BJ-5ta, HDF and SJD.1 primary fibroblasts were obtained from two independent assays with six technical replicates for each treatment.

2.5. Scratch assay

To evaluate the effects of the PS-NPs on fibroblast cell migration a classical scratch assay was performed as described in (Félix et al., 2021; Letsiou et al., 2020). For this assay, BJ-5ta, HDF and SJD.1 fibroblast cells from passage 2–3 were used. Briefly, each cell line was seeded into 24-well tissue culture plates (75,000 cells/well) in cell specific medium and incubated overnight to permit cell adherence. After overnight incubation, the medium was replaced with cell specific medium supplemented with PS-NPs of different sizes (50, 500 and 1000 nm) and at different concentrations (0.1, 1 and 10 μg/ml) and the cells were incubated for 72 h under optimal temperature and oxygen conditions. The control group of each cell line was treated with complete medium without PS-NPs. After incubation, the medium was removed, and cells were washed with PBS to remove the PS-NPs that had not been taken up by the cells.

Multiple scratches were made in the confluent cell monolayer in each well using a 200 μl micropipette tip so that approximately 50 % of the adherent cells were removed (Félix et al., 2021). After scratching, the cells were washed twice with PBS to remove the detached cells, complete medium was added to the cells and the cells were incubated under optimal conditions. The evolution of scratch repair was captured with black and white digital images using a Leica DM IL microscope coupled to a Visicam PRO 20C digital camera. Photographs were analyzed using ImageJ software for the calculation of the repaired area. Photos of BJ-5ta and SJD.1 fibroblast scratch repair were captured at 0 h immediately after scratching and at 12 h and 24 h after inflicting a scratch. For HDF fibroblasts photos were taken at 0 h immediately after scratching and at 12 h and 30 h after inflicting a scratch. The scratch recovery area was obtained using the results from three technical replicates carried out in two independent assays for each test group.

2.6. Cell activity assays

2.6.1. Oxidative stress assay

ROS production in BJ-5ta, HDF and SJD.1 cells was determined using a DCFH-DA ROS assay kit (BQCKit, Bioquochem, Spain), according to the manufacturer's instructions. For these assays, cells were seeded into 96-well tissue culture plates (50,000 cells/well) and allowed to adhere overnight. After cell adherence, the cell specific medium was replaced with cell specific medium supplemented with PS-NPs of different sizes (50, 500 and 1000 nm) and at different concentrations (0.001, 0.01, 0.1, 1 and 10 μg/ml), and the cells were incubated for 72 h under optimal conditions. A negative control (medium alone) and a positive control (medium supplemented with 1 μl of 55 mM tert-butyl hydroperoxide 4 h before performing the assay) were prepared for each cell line assayed. DCFDA-DA assay results were measured using a multiplate reader at Ex/Em = 485/535 nm (TECAN Infinite M200 Plate Reader, Switzerland), following the manufacturer's instructions. The results are shown as the average ± SEM of six technical replicates and two independent experiments.

2.6.2. Apoptosis assay

Apoptosis of BJ-5ta, HDF and SJD.1 cells was determined using a Caspase-2 Fluorometric assay kit (BQCKit, Bioquochem, Spain) following the manufacturer's instructions. This assay measures the activity of caspases that recognize the sequence VDVAD. For this assay, each cell line was seeded into 96-well tissue culture plates at a density of 50,000 cells/well and incubated overnight under optimal conditions for cell adherence. After cell adherence, the medium was replaced with cell specific medium supplemented with PS-NPs, and the cells were incubated for 72 h. A negative control (complete medium only) and a

positive control (complete medium supplemented with 1 μl of 55 mM tert-butyl hydroperoxide, 2 h before performing the assay) was included in each of the assays. The test groups were treated with medium supplemented with PS-NPs of different sizes (50, 500 and 1000 nm) and a range of concentrations (0.001, 0.01, 0.1, 1 and 10 μg/ml). Caspase-2 assays were measured using a multiplate reader at Ex/Em = 430/480 (TECAN Infinite M200 Plate Reader, Switzerland) following the manufacturer's instructions. Relative caspase-2 activity was calculated as follows:

$$\text{Relative fold change caspase} - 2 \text{ activity} = (F_{It} - F_{Inc})/(F_{Ic} - F_{Inc}).$$

where F_{it} represents the mean value of the measured fluorescence intensity of the test item (including the positive control), F_{Ic} represents the mean value of the measured fluorescence intensity of the control, and F_{Inc} represents the mean value of the measured fluorescence intensity of the negative control. The results are shown as the average ± SEM of six technical replicates and two independent experiments.

2.6.3. Alkaline phosphatase and acid phosphatase assays

Alkaline phosphatase (ALP) catalyzes the hydrolysis of phosphate esters and produces organic radicals and inorganic phosphate. For this assay, cells (BJ-5ta, HDF and SJD.1) were seeded into 96-well tissue culture plates (50,000 cells/well) in cell specific medium and incubated overnight until cell adherence. After cell adherence the medium was removed, and cell specific medium containing PS-NPs (1000 nm, 1 μg/ml) was added, and the cells were incubated for 72 h. The control group for each cell line was incubated in medium without PS-NPs and a negative control (medium only) was included in all assays. The experiments were performed with six technical replicates and in two independent experiments. An alkaline phosphatase assay kit (Abcam, ab83371) was used to measure cell ALP activity using a multiplate reader (TECAN Infinite M200 Plate Reader, Switzerland) and measuring the fluorescence intensity (Ex/Em = 360/440 nm), according to the manufacturer's instructions.

An acid phosphatase assay kit (Abcam, ab83370) was used to measure cell AP activity following the manufacturer's instructions. For this assay, cells (BJ-5ta, HDF and SJD.1) were seeded into 96-well tissue culture plates (50,000 cells/well) in cell specific medium and incubated overnight until cell adherence. After cell adherence medium was replaced with cell specific medium containing PS-NPs (1000 nm, 1 μg/ml), and the cells were incubated for 72 h under optimal conditions. A control was included for each cell line and consisted of the cells in medium without PS-NPs and a negative control that contained medium only. The experiment was set up with six technical replicates and two independent experiments were carried out.

AP activity was determined following the manufacturer's instructions after washing cells to remove PS-NPs. Activity was measured using a multiplate reader (Ex/Em = 360/440 nm) (TECAN Infinite M200 Plate Reader, Switzerland) according to the manufacturer's instructions.

2.7. Statistical analysis

In this study, data are presented as average ± standard error of the mean (SEM). Statistical analyses were performed using GraphPad Prism version 7.0a software. All data was tested and passed normality with GraphPad Prism normality and lognormality tests, and thus parametric statistical analysis was performed. A two-tailed Student's *t*-test was used to compare the treatment groups with the control group in PS-NP uptake, cell proliferation, scratch assay, MTT assay, ALP and AP assays. For oxidative stress and apoptosis assay results, a two-way analysis of variance (ANOVA) followed by a Tukey's Multiple Comparison test was performed. A *p*-value <0.05 (*) was considered to indicate statistical significance.

Principal component analysis (PCA) was performed for exploratory data analysis and to verify the similarities between the samples and the relationship of the cell activity assays with discrete features. PCA analysis was carried out using Rstudio (version 3.1.6) with the psych (Revelle, 2016), reshape2 (Wickham, 2012), factoextra (Kassambara and Mundt, 2017) and ggplot2 (Wickham, 2016) packages. All data used for PCA analysis were normalized under the default parameters of the software. The PCA analysis was performed with the results (average of $n = 2$ assays with 6 technical replicates) for the five cell activities measured (MTT, ROS, caspase-2, ALP and AP) and the three cell lines in the control and PS-NP treated groups (1000 nm, 1 μg/ml).

3. Results

3.1. Skin fibroblast origin affects the cellular uptake of PS-NPs

Human BJ-5ta, HDF, and zebrafish SJD.1 fibroblasts are adherent cells that, when in high concentrations, form confluent monolayers. Observations of the morphology of HDF cells revealed they are larger than the BJ-5ta and SJD.1 cells. The SJD.1 cell line exhibited a substantially different morphology and was much smaller than the other cell lines (Fig. 2a). When incubated with 1 μg/ml of 1000 nm PS-NPs for 72 h, all the studied cell lines accumulated a significant number of PS-NPs (Fig. 2a) and SJD.1 accumulated the highest number of PS-NPs, followed by HDF, and BJ-5ta (Fig. 2b). Our observations also indicated that after uptake, the PS-NPs remained in the cytoplasm, surrounding the cell nucleus.

3.2. PS-NPs exposure has a detrimental effect on cell viability

The viability of BJ-5ta cells decreased significantly following pre-incubation with PS-NPs ($p < 0.05$). Our results demonstrated that cell viability decreased continuously and significantly ($p < 0.05$) as the concentration of PS-NPs increased (0.001 μg/ml to 10 μg/ml) for the three PS-NP sizes tested, 50, 500 and 1000 nm (Fig. 3). Only in the 500 nm and 1000 nm NPs at 0.001 μg/ml, was the viability of BJ-5ta cells similar to the control.

The lower concentrations (0.001 μg/ml and 0.01 μg/ml) of all sizes of PS-NPs (50 nm, 500 nm and 1000 nm) did not significantly affect the viability of HDF cells. The HDF cell viability was significantly decreased ($p < 0.05$) when they were pre-incubated with 50 nm PS-NPs at 1 and 10 μg/ml and with 500 nm and 1000 nm PS-NPs at 0.1–10 μg/ml.

Compared to the control the pre-incubation of SJD.1 cells with PS-NPs (50 nm, 500 nm and 1000 nm) did not significantly affect cell viability apart from at 10 μg/ml. SJD.1 cells pre-incubated with 1000 nm PS-NPs at 1 μg/ml also had a significantly reduced ($p < 0.05$) cell viability compared to the control.

3.3. PS-NP size and concentration affect skin fibroblast proliferation

Our results showed that control and PS-NP treated cells increased in number over time, but that cells pre-incubated with PS-NPs had a significantly reduced ($p < 0.05$) proliferation. In general, BJ-5ta cells had the highest rate of proliferation, followed by SJD.1 cells and HDF cells (Fig. 4). Among all the fibroblast cell lines exposed to different sizes of PS-NPs, it was the largest particle size tested, 1000 nm, that exhibited the most significant effect on cell proliferation.

The proliferation of BJ-5ta cells was not affected by 50 nm PS-NPs. Proliferation was significantly inhibited ($p < 0.05$) from 48 h onwards in BJ-5ta fibroblasts pre-exposed to 500 nm NPs at 0.01 μg/ml, 0.1 μg/ml, 1 μg/ml. After 120 h in 500 nm PS-NP treated cells the inhibitory effect on BJ-5ta proliferation was significantly higher than the same size PS-NPs but at a lower concentration (0.01 μg/ml). Pre-incubation of BJ-5ta with 0.01 μg/ml 1000 nm PS-NPs, caused a significant inhibition of BJ-5ta cell proliferation after 120 h and at higher PS-NP concentrations (0.1 μg/ml and 1 μg/ml) a significant inhibition ($p < 0.01$) of proliferation was detected at 48 h, and the inhibitory effect was more evident at higher PS-NP concentrations.

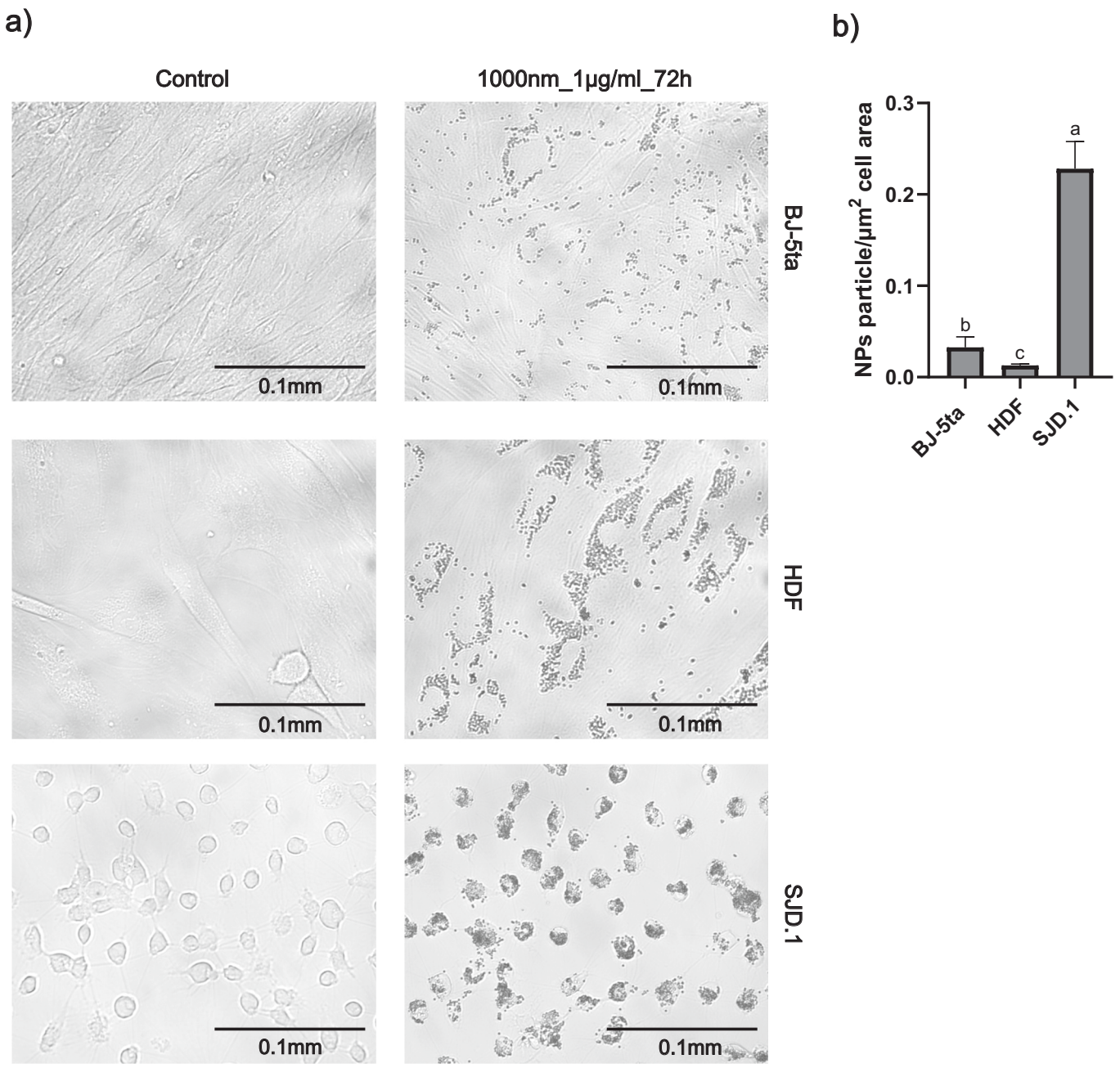

Fig. 2. Morphological observation of fibroblast cell lines with and without PS-NPs (1000 nm at 1 μg/ml). (a) Changes in cell morphology were observed after 72 h incubation with PS-NPs. Photos were taken with a Leica DM IL microscope coupled to a PRO 20C digital camera. Scale bars in photographs represent 100 μm. (b) A graphical representation of the number of PS-NPs taken up by cells was determined using image J. The results are shown as the average ± SEM of six technical replicates in two independent experiments. Data were analyzed using a two-way ANOVA followed by a Tukey's Multiple Comparison test. The statistical analysis was performed using GraphPad Prism version 7.0a. A $p < 0.05$ (*) was considered significant.

The proliferation of HDF cells was not affected by pre-incubation with 50 nm PS-NPs except at a concentration of 1 μg/ml at 168 h when significant inhibition ($p < 0.05$) was observed. HDF cell proliferation was not affected by 500 nm PS-NPs at 0.01 μg/ml. The pre-incubation of HDF cells with 0.1 μg/ml and 1 μg/ml 500 nm PS-NPs, significantly inhibited proliferation after 96 h ($p < 0.05$), and the inhibitory effect increased with time. The inhibition of HDF proliferation was more pronounced for 1 μg/ml 500 nm PS-NPs than for 0.1 μg/ml. Pre-incubation of HDF cells with 1000 nm PS-NPs, significantly inhibited ($p < 0.05$) the proliferation of HDF cells at all concentrations and timepoints used except for 0.01 μg/ml, which did not significantly inhibit proliferation at 48 h. From 96 h onwards, the higher the PS-NP concentration, the more intense the inhibitory effect on the proliferation of HDF cells.

The proliferation of SJD.1 cells was not significantly affected by pre-incubation with 50 or 500 nm PS-NPs irrespective of the concentration. Pre-incubation of SJD.1 cells with 1000 nm PS-NPs at 0.1 μg/ml, caused a significant inhibition ($p < 0.05$) of proliferation after 168 h, and PS-NPs at 1 μg/ml caused a significant inhibition ($p < 0.05$) of proliferation after 120 h.

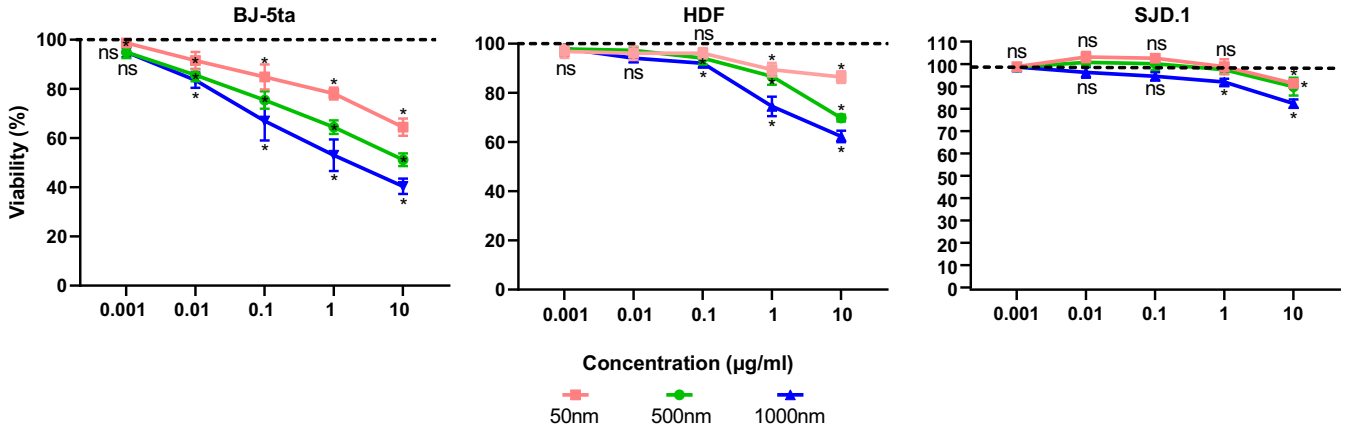

Fig. 3. Effect of PS-NP exposure on fibroblast cell viability. Cell viability was determined for BJ-5ta, HDF and SJD.1 fibroblast cells that had been exposed to PS-NPs of different sizes (50 nm, 500 nm and 1000 nm) and concentrations (0.001 μg/ml, 0.01 μg/ml, 0.1 μg/ml, 1 μg/ml and 10 μg/ml) using an MTT assay after incubation of the cells with PS-NPs for 72 h. The results are shown as the average ± SEM of six technical replicates for each treatment group in two independent experiments. The data were analyzed by comparing the treatment group and the control using a two-tailed Student's *t*-test. Statistical analysis was performed using GraphPad Prism version 7.0a. $p < 0.05$ was considered significant and is identified with (*).

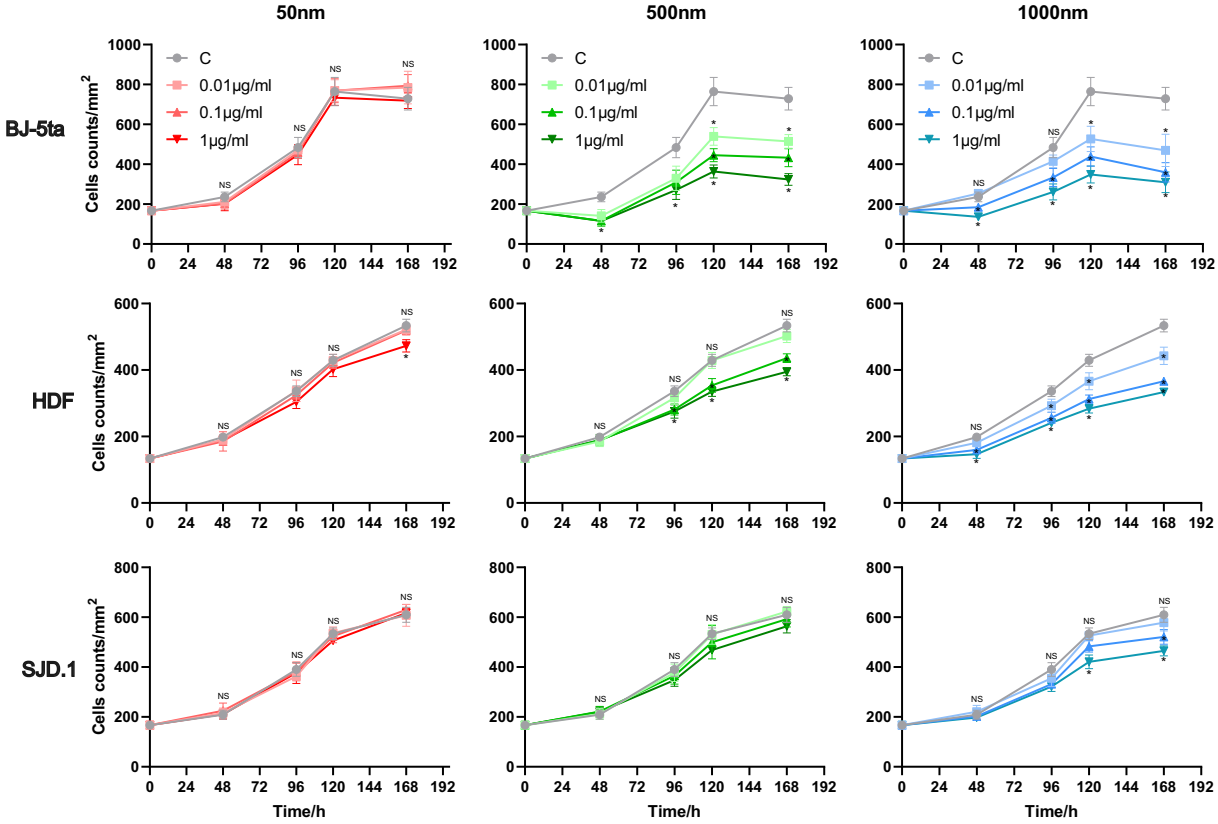

Fig. 4. The effect of PS-NP size and concentration on BJ-5ta, HDF and SJD.1 cell proliferation across time. The effect of PS-NPs of different sizes (50, 500 and 1000 nm) and concentrations (0.01, 0.1 and 1 μg/ml) on the proliferation of human (BJ-5ta and HDF) and fish (SJD.1) fibroblast cells. Cells were counted at 48 h intervals across 168 h after seeding. The results are displayed as the average ± SEM of six technical replicates in two independent experiments. The data were analyzed using a two-tailed Student's t-test between the PS-NP exposed cells and the control cells. The statistical analysis was performed using GraphPad Prism version 7.0a. $p < 0.05$ was considered significant and is identified with *.

3.4. PS-NP exposure modifies skin fibroblast migration and scratch recovery

Scratch repair assays were performed with BJ-5ta fibroblasts after pre-incubation with 50 and 500 and 1000 nm PS-NPs (Supplementary Fig. 2). BJ-5ta cells exposed to 50 nm PS-NPs at 0.1 μg/ml, 1 μg/ml and 10 μg/ml and 500 nm at 0.1 μg/ml did not show a significant enhancement or change in scratch repair compared to the control cells. By 24 h after damage approximately 96–98 % of scratch recovery (expressed as % of the total scratch area at time 0) was achieved irrespective of the concentration of PS-NPs (Fig. 5). The scratch repair was slower in BJ-5ta cells exposed to 500 nm PS-NPs at 1 μg/ml and 10 μg/

ml compared to the control BJ-5ta cells. Scratch repair by BJ-5ta cells exposed to 500 nm PS-NPs at 1 μg/ml was significantly inhibited ($p < 0.05$) 24 h after the scratch and 500 nm PS-NPs at 10 μg/ml caused an even more pronounced inhibition of scratch repair at both 12 h and 24 h ($p < 0.05$). For 500 nm pre-exposed BJ-5ta cells, approximately 97 %, 82 % and 58 % of scratch recovery was achieved 24 h after scratching in cells pre-incubated with 0.1 μg/ml, 1 μg/ml and 10 μg/ml PS-NPs, respectively. Scratch repair in BJ-5ta cells pre-incubated with 1000 nm PS-NPs at 0.1 μg/ml, 1 μg/ml and 10 μg/ml was significantly inhibited at all time points ($p < 0.05$). For BJ-5ta cells treated with 1000 nm PS-NPs, approximately 89 %, 74 % and 55 % of scratch recovery compared to the control cells was achieved 24 h after scratching in 0.1 μg/ml, 1 μg/ml and 10 μg/ml PS-NPs, respectively.

HDF fibroblasts cells were also considered in scratch repair assays, and recovery was monitored at 12 and 30 h after the scratch (Supplementary Fig. 2). In HDF cells pre-incubated with 50 nm PS-NPs at 0.1 μg/ml, 1 μg/ml, 10 μg/ml, no significant change in scratch recovery was observed when compared to the control group, and approximately 89–97 % of scratch recovery (expressed as % of the total scratch area at time 0) was achieved 30 h after scratching (Fig. 5). The HDF cell scratch repair was significant inhibited ($p < 0.05$) at 30 h when cells had been pre-incubated with 500 nm PS-NPs at 0.1 μg/ml, 1 μg/ml, 10 μg/ml and cells achieved approximately 92 %, 82 %, and 63 % scratch recovery, respectively compared to the control. Pre-incubation of HDF cells with 0.1 μg/ml, 1 μg/ml, 10 μg/ml of 1000 nm PS-NPs, significantly inhibited scratch recovery ($p < 0.05$) compared to the control HDF cells and in PS-NP exposed HDF cells approximately 63 %, 45 %, and 19 % recovery occurred, respectively at 30 h.

Scratch repair assays were performed using SJD.1 primary fibroblasts pre-incubated with PS-NPs and then monitored at 12 and 24 h after the scratch (Supplementary Fig. 2). Scratch recovery was not significantly different from the control in SJD.1 cells pre-incubated with 50 nm PS-NPs at 0.1 μg/ml, 1 μg/ml, 10 μg/ml, and approximately 92–97 % scratch recovery (expressed as % of the total scratch area at time 0) was achieved 24 h after scratching (Fig. 5). SJD.1 primary fibroblasts pre-incubated with 500 nm PS-NPs at 1 μg/ml and 10 μg/ml had a significantly slower ($p < 0.05$) rate of scratch repair compared to the control. Pre-incubation of SJD.1 cells to 500 nm PS-NPs at 0.1 μg/ml, 1 μg/ml, and 10 μg/ml had a scratch recovery of 95 %, 91 %, and 84 % 24 h after scratching, respectively. The 1000 nm PS-NPs at 0.1 μg/ml, 1 μg/ml, and 10 μg/ml significantly inhibited scratch recovery by SJD.1 cells at 12 h and 24 h ($p < 0.05$) after the scratch. SJD.1 cells treated with 1000 nm PS-NPs at 0.1 μg/ml, 1 μg/ml, and 10 μg/ml achieved approximately 90 %, 72 %, and 64 % scratch recovery 24 h after scratching, respectively.

3.5. PS-NPs alter skin fibroblast cell activity

3.5.1. ROS activity

The ROS activity of BJ-5ta cells was not significantly affected by PS-NPs (50 nm, 500 nm, and 1000 nm) at 0.001–0.1 μg/ml (Fig. 6a). A significant increase ($p < 0.05$) in BJ-5ta cell ROS activity occurred when cells were pre-incubated with PS-NPs (50 nm, 500 nm, and 1000 nm) at 1 μg/ml (the larger the PS-NPs the larger the increase in ROS). The pre-incubation of BJ-5ta cells with PS-NPs (50 nm, 500 nm and 1000 nm) at 10 μg/ml caused a significant reduction ($p < 0.05$) in ROS enzyme

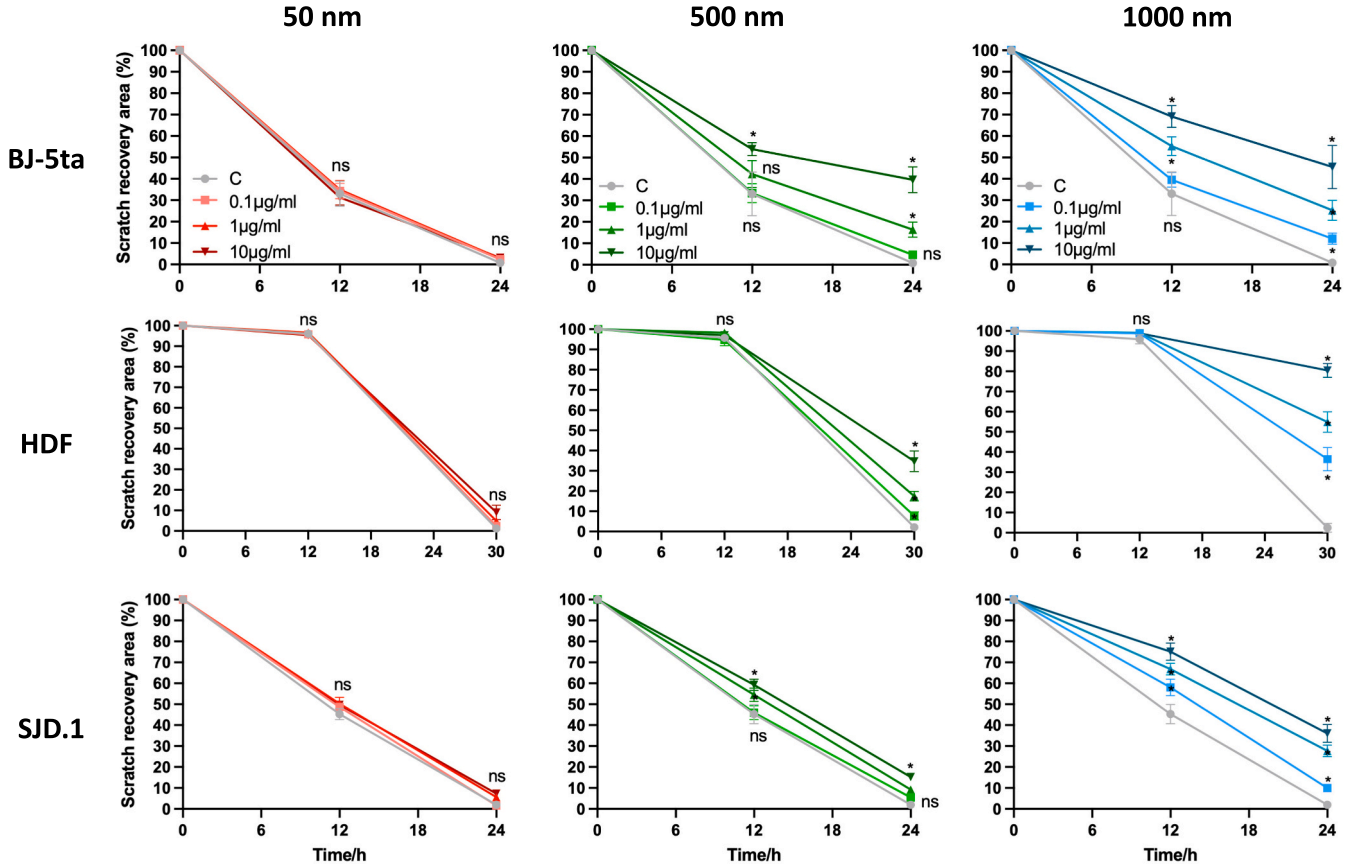

Fig. 5. The effect of PS-NPs on scratch repair. A graphical representation of the scratch recovery area (percentage) measured at 0 h, 12 h and 24 h for BJ-5ta and SJD.1 and at 0 h, 12 h and 30 h for HDF cells in relation to the area immediately after the scratch was made (taken as 100 %). The results are shown as the average ± SEM of three technical replicates for each treatment group in two independent experiments. The data were analyzed using a two-tailed Student's t-test and comparing each of the treatment groups and the control. The statistical analysis was performed using GraphPad Prism version 7.0a. $p < 0.05$ was considered significant and is identified with *.

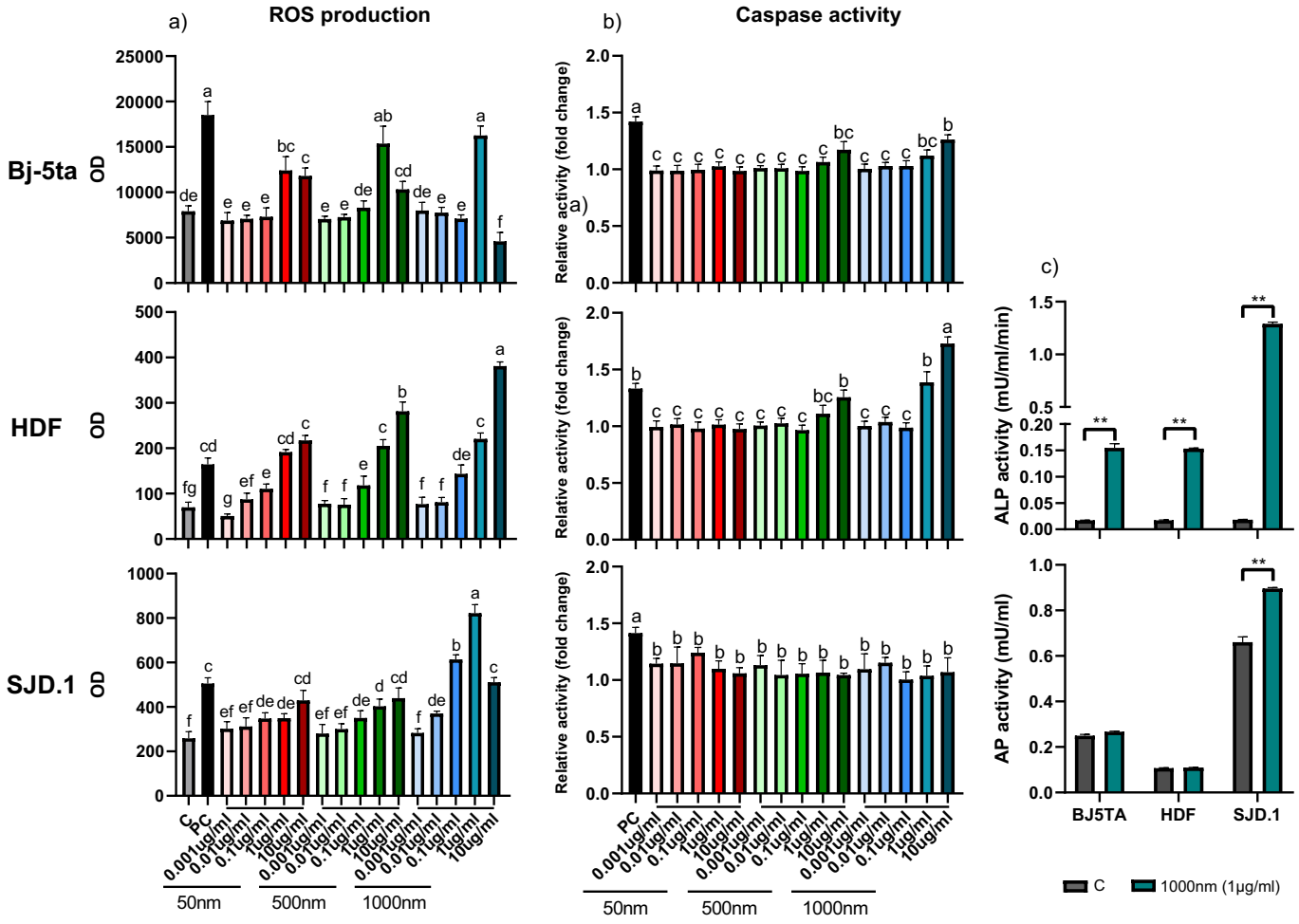

Fig. 6. Effects of PS-NPs on fibroblast cell activity. The activity level of ROS production and apoptosis was determined for BJ-5ta, HDF and SJD.1 fibroblast cells that had been exposed to PS-NPs of different sizes (50 nm, 500 nm and 1000 nm) and concentrations (0.001 μg/ml, 0.01 μg/ml, 0.1 μg/ml, 1 μg/ml and 10 μg/ml), a) ROS production was measured by determining DCFH-DA in fibroblast cells after incubation of the cells with PS-NPs for 72 h. "C" and "PC" in the figure represent the control and positive control groups, respectively. b) Apoptosis was measured by determining the activity of Caspase 2 in fibroblast cells after incubation of the cells with PS-NPs for 72 h. The "PC" group in the figure represents the positive control. The results are shown as the average ± SEM of six technical replicates for each treatment group in two independent experiments. The data were analyzed using a two-way ANOVA followed by a Tukey's Multiple Comparison test. c) ALP and AP enzyme activities were measured in fibroblast cells exposed to 1000 nm PS-NPs at a concentration of 1 μg/ml for 72 h. The results are shown as the average ± SEM of six technical replicates for each treatment group in two independent experiments. The data were analyzed using a two-tailed Student's t-test between the treatment group and the control. The statistical analysis was performed using GraphPad Prism version 7.0a. $p < 0.05$ was considered significant and significantly different groups were identified using different letters (a, b) in ROS and apoptosis results and with * for ALP and AP results.

activity and the larger the PS-NPs the larger the decrease in ROS.

No significant changes in ROS activity occurred in HDF cells pre-incubate with PS-NPs (50 nm, 500 nm and 1000 nm) at 0.001–0.01 μg/ml. HDF cells pre-incubated with PS-NPs (50 nm, 500 nm and 1000 nm) at 0.1–10 μg/ml had a significantly increased ($p < 0.05$) ROS activity compared to the control cells.

ROS activity did not change in SJD.1 cells pre-incubated with PS-NPs (50 nm and 500 nm) at 0.001–0.01 μg/ml. PS-NPs of 50 nm and 500 nm at 0.1–10 μg/ml caused a significant increase ($p < 0.05$) in ROS activity in SJD.1 cells. PS-NPs of 1000 nm at 0.001 μg/ml did not change ROS activity in SJD.1 cells but concentrations between 0.01 and 10 μg/ml caused a significant increase ($p < 0.05$) compared to the control SJD.1 cells.

3.5.2. Caspase 2 enzyme activity

Caspase 2 enzyme activity was not significantly different in BJ-5ta cells pre-incubated with any size or concentration of PS-NPs apart from 10 μg/ml PS-NPs of 1000 nm where it was significantly increased ($p < 0.05$) (Fig. 6b). HDF cells pre-incubated with 500 nm (1 μg/ml) and 1000 nm (1 and 10 μg/ml) PS-NPs had significantly higher ($p < 0.05$) Caspase 2 enzyme activity. PS-NP exposure at any size or concentration did not significantly change Caspase 2 enzyme activity in SJD.1 cells.

3.5.3. ALP and AP enzyme activity

ALP enzyme activity was significantly increased ($p < 0.05$) in BJ-5ta and HDF cells pre-incubated with 1000 nm PS-NPs at 1 μg/ml. AP enzyme activity was not affected in BJ-5ta and HDF cells by PS-NP exposure (Fig. 6c). Both ALP and AP were significantly increased ($p < 0.05$) in SJD.1 cells exposed to 1000 nm PS-NPs at 1 μg/ml.

3.6. The predominant changes in cell activity determined by PCA

PCA analysis revealed that 93.6 % of the overall variance was explained by the PS-NPs of 1000 nm at a concentration of 1 μg/ml (Fig. 7). Analysis of the results for all the cell lines pre-incubated with PS-NPs revealed, Dimension 1 (Dim1) contained 63.5 % of the overall variance, and that the separation of the human (BJ-5ta and HDF) and fish (SJD.1) cell lines was due to the AP, ALP, and MTT activity.

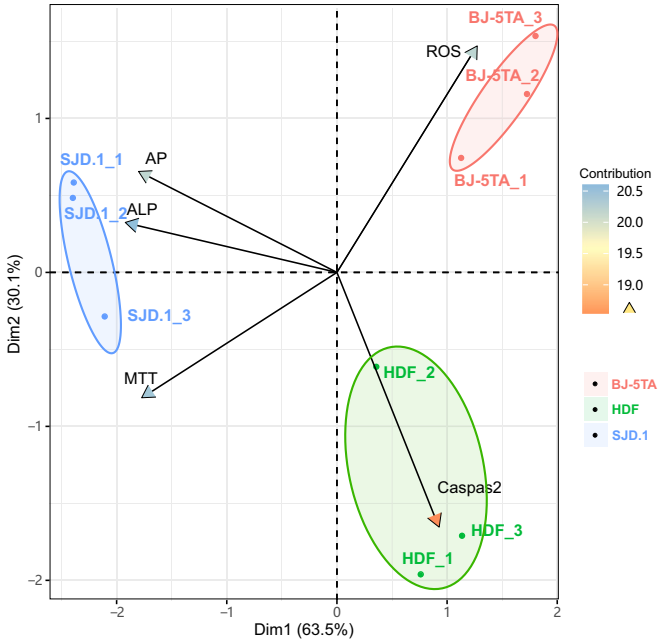

Fig. 7. Principal component analysis (PCA) to determine the principal effects of PS-NPs on the enzyme activity of human (HDF and BJ-5ta) and fish (SJD.1) fibroblast cells. The biplot originated from PCA is shown and the analysis integrated all measured variables (MTT, ROS, Caspase2, ALP and AP) and the three fibroblast cell lines (BJ-5ta, HDF and SJD.1) exposed to 1000 nm PS-NPs at 1 μg/ml. Different colors represent the different cell lines used in the experiments after incubation with PS-NPs for 72 h, and each ellipse represents the 0.95 confidence range. Variables (activity) are represented by black line segments passing through the axis dots. The color inside the arrowhead for each projection indicates the contribution of the variables and the heatmap (right hand side) indicates their contribution.

Specifically, SJD.1 cells exhibited increased AP, ALP, and MTT activities, while ROS and Caspase 2 activities decreased, and ROS was negatively correlated with AP and ALP. Dim2 contained 30.1 % of the overall variance, and the separation of the human newborn male (BJ-5ta) and adult female (HDF) cell lines was due to differences in ROS and Caspase 2. Notably, PS-NPs led to faster changes in ROS in BJ-5ta cells, while in HDF cells Caspase 2 activity changed faster.

4. Discussion

Aquatic systems are a major destination for environmental nanoplastics, which puts humans, fish and other aquatic organisms at risk. While there are an increasing number of *in vivo* studies of PS-NPs in fish and humans, research focused on barrier tissues like skin is scarce. In this study, we investigated the uptake capacity of PS-NPs by human and fish skin fibroblast cell lines. Our results showed that all fibroblast cell lines were able to uptake PS-NPs and they accumulated in the cytoplasm surrounding the cell nucleus. Our findings are supported by a recent study on murine primary skin cells exposed to PS-NPs, where efficient cellular uptake of NPs of several sizes (ranging from 200 nm to 6 μm) was observed after 24 h of incubation (Schmidt et al., 2023). A key observation of our study was that exposure of human adult dermal fibroblasts (HDF) and infant fibroblasts (BJ-5ta) to 500 and 1000 nm PS-NPs at relatively low concentrations compared to previous studies (0.01/0.1 μg/ml - 1 μg/ml for 72 h) significantly inhibited proliferation. This compliments observations made in another human foreskin fibroblast cell line (Hs27) where exposure to 5, 25 and 75 μg/ml of 100 nm PS-NPs for 48 h significantly inhibited cell proliferation (Poma et al., 2019). Additionally, a study with an intestinal epithelial cell line (HIEC-6) and three human colon carcinoma cell lines (RKO, HT-29, and HCT-116) showed that exposure to 50 and 100 μg/ml of 100 nm PS-NPs for 48 h also inhibited cell proliferation (Xu et al., 2023). Furthermore, the results of these studies hint at a cell-specific response since HIEC-6 and Hs27 cell proliferation was inhibited by PS-NPs sooner (at 24 h) than for the other cell types. The results of our study with 3 different types of skin fibroblasts revealed a clear relationship between PS-NP particle size and concentration and the inhibition of proliferation. It is worth noting that, as the size and concentration of the PS-NPs increased, the inhibitory effect on fibroblast proliferation became more pronounced. Understanding the underlying mechanisms responsible for this phenomenon and how size specifically influences the impact of PS-NPs on cells needs further exploration. Moreover, when comparing the three skin fibroblast cell lines in terms of PS-NP exposure time, concentration, and size, it was found that the inhibitory effect of NPs on proliferation was greater for human skin fibroblasts than for fish fibroblasts where only PS-NP of 1000 nm had a significant effect.

The reason for the variability in the proliferative response of different cell lines to PS-NPs has not previously been reported but we hypothesize it may be related to the basal rate of cell proliferation since the BJ-5ta cells (fibroblasts from infant foreskin) that proliferate faster and exhibit higher motility were more significantly inhibited by PS-NPs than adult HDF cells. Furthermore, a study involving rheumatic arthritis - fibroblast-like synoviocytes (RA-FLS) demonstrated that MPs promoted proliferation and increased migration capacity of RA-FLS, and this effect was proposed to be explained by the tumor-like characteristics of RA-FLSs (Lihua and Zhiyin, 2023). Taken together, these findings provide further support for our hypothesis that the effects of PS-NPs depend on particle size, and concentration but is also highly dependent on the specific characteristics of the cells involved.

Insights into the mechanistic basis of the divergence in the cell type response to PS-NP exposure may be explained in part by the Caspase 2 activity. For example, proliferation of fish fibroblasts was not significantly affected by PS-NP exposure, and Caspase 2 activity, an indicator of apoptosis, was not significantly changed by PS-NP exposure. In contrast, in human cell lines, as the size and concentration of the PS-NPs increased, the proliferation significantly decreased but the activity of Caspase 2 did not change in the same PS-NPs concentrations. This suggests that PS-NPs inhibited cell proliferation but did not significantly affect apoptosis in PS-NP exposed human fibroblast cells. These findings provide two noteworthy insights: 1) the pathways of proliferation and apoptosis in zebrafish skin fibroblasts under PS-NP exposure may differ from those of human skin fibroblasts, and 2) fibroblast cells originating from adult and infant skin within the same species exhibit differences in the apoptotic pathway under PS-NP exposure. In experiments with rat ovarian granulosa cells exposed to PS-MPs the NLRP3/Caspase-1 signaling pathway was responsible for triggering pyroptosis and apoptosis and not Caspase 2, which we measured in our study (Hou et al., 2021). Similarly, when rat basophilic leukemia (RBL-2H3) cells were exposed to either PS-MPs or PS-NPs the organelles were damaged and this promoted MOAP-1 induced apoptosis (Liu et al., 2022). This highlights that in cell-based studies caution is needed in the interpretation of apoptosis results since the pathway may be cell dependent and, in many studies, only a single apoptosis pathway is studied. The results from the cell proliferation analysis in the present study indicate that the response of fibroblasts under PS-NP exposure was species-specific and depended on the origin of the cell line. Furthermore, taking into consideration the results obtained for different human skin fibroblasts it is possible age and sex influenced the response to PS-NPs.

Fibroblasts play a crucial role in wound healing as they are responsible for synthesizing extracellular matrix components and promoting tissue remodeling (Braff and Gallo, 2006; Eming et al., 2014; Rodrigues et al., 2019). The scratch repair assay gives insight into the cellular and molecular mechanisms underlying a critical process in skin, wound healing. In assessment of wound healing fibroblast migration in response to damage is quantified, and generally core genes, proteins and signaling pathways involved in this process are quantified (Félix et al., 2021;

Letsiou et al., 2020). *In vitro* assays of scratch repair in previous studies has revealed that the involvement of actin in cell protrusion, contraction, and retraction movements is similar in human dermal fibroblasts and the zebrafish SJD.1 primary fibroblasts (Etienne-Manneville, 2013, 2004; Félix et al., 2021; Garcin and Straube, 2019; Letsiou et al., 2020). In our study, the presence of PS-NPs inside fibroblasts negatively affected their migration in a time-, size- and concentration-dependent manner. The results with skin fibroblasts indicated that the bigger PS-NPs at higher concentrations caused more significant inhibition of cell migration. The severity of the effect of PS-NPs on the migration of the cell types used in the present study was like the cell proliferation studies with a more pronounced effect on human skin fibroblasts compared to fish fibroblasts. Taking together the outcome of the cell proliferation and cell viability assays in the presence of PS-NPs it appears that the differences in cell migration among species and even cell types may be related to the inhibition of cell proliferation. In other words, PS-NP exposure caused a deceleration in proliferation of human skin cells and presumably this resulted in a lower number of cells participating in scratch repair. This was particularly evident in the case of cells pre-incubated with 50 nm PS-NPs, which did not affect cell migration but did cause decreased cell viability.

Cell proliferation seems to be particularly sensitive to PS-NP exposure and Jeong et al. (2022) reported that, although PS-NPs inhibited stem cell proliferation, they did not significantly affect their future differentiation or other essential functions. The results of our study are in concordance with this study since although PS-NPs negatively impacted cell proliferation they had only a limited effect on the capacity of skin fibroblasts to migrate. In fact, immunohistochemical and cell painting studies (personal observation) revealed that PS-NPs were not associated with the cytoskeleton or microtubules in the fibroblast cells. Nonetheless, of note was the observation that smaller dimension PS-NPs (50 nm) did not have an appreciable effect on fibroblast proliferation during the "S" phase of the fibroblast proliferation curve or on the migration of either human or fish skin fibroblasts.

Studies of PS-NP uptake and the associated consequences are well represented in the existing literature but relatively few studies have assessed the capacity of cells to eliminate PS-NPs. One study reported the release of 44 nm PS-NPs from bovine oviductal epithelial cells and human colon fibroblasts after a 4 h incubation in fresh culture medium (Fiorentino et al., 2015). This raises interesting questions about the factors underlying the lesser effects observed for smaller dimension PS-NPs in our study since excess PS-NPs were removed by washing the cells before measuring their response. We did not determine in our study if the cells eliminated the PS-NPs they took up and this aspect requires further investigation. Nonetheless, it should be noted that PS-NPs of 50 nm still exhibited cytotoxic effects on skin fibroblasts, reduced cell viability and increased the production of ROS. Similarly, in human alveolar type II lung epithelial cells (A549) exposure to PS-NPs of 25 nm was reported to reduce their viability (Xu et al., 2019).

Although ROS plays critical roles in cell signaling and defense, excessive production or impaired removal can induce oxidative stress and cell damage (Elsayed Azab et al., 2019). The time-, size- and concentration-dependent pattern of PS-NP cytotoxicity in our study was coherent with the observations in human intestinal epithelial Caco-2 cells that larger particles of PS-NP at higher concentrations induced a greater production of ROS (Cortés et al., 2020; Wu et al., 2019). Our findings are further supported by the results of a recent study on murine primary skin cells, which showed that small sized PS-NPs (200 and 1000 nm) did not significantly increase ROS (Schmidt et al., 2023).

A surprising observation that remains to be explained is the significantly lower cytotoxicity of PS-NPs on fish skin fibroblasts. The limited effect of PS-NPs of a small size (<1000 nm) on fish fibroblast (SJD.1) proliferation, migration and cytotoxicity *in vitro* raises interesting questions about the consequences and risks from PS-NP (<1000 nm) pollution in aquatic environments. Nonetheless, the significant increase in ALP and AP enzyme activity in fish fibroblasts when exposed to 1 μg/ml PS-NP was indicative of a cellular response. ALP plays a role in the synthesis and organization of the extracellular matrix (ECM), cell signaling, and differentiation most of which were not evaluated in our study (Shekaran and García, 2011; Shen et al., 2022). However, scratch repair (analogous to wound healing in which ALP has a role) was assessed and revealed that ALP activity was highly and significantly increased in PS-NP exposed fish and human fibroblasts, which is the expected response (Krötzsch et al., 2008). Nonetheless, despite the increased ALP activity caused by PS-NP exposure, contrary to expectations the migration of fish and human fibroblasts was significantly reduced (Figs. 4, Supplementary Fig. 2). The results for ALP activity and SDJ.1 migration clearly reveal the importance of both *in vitro* and *in vivo* studies to fully understand the likely consequences to fish of NP exposure.

The precise function of AP in skin fibroblast cells is not well established but the enzyme is primarily localized within lysosomes and functions as a hydrolase enzyme. AP plays an important role in the breakdown of diverse molecules, including proteins, nucleic acids, and carbohydrates, enabling efficient recycling of cellular components (Bull et al., 2002; Filomeni et al., 2015). Additionally, AP is involved in cellular phosphate metabolism, contributing to the maintenance of phosphate homeostasis and participating in various cellular processes that rely on phosphate, such as energy metabolism, signaling, and biomolecule synthesis (Anand and Srivastava, 2012). The significant increase in AP enzyme activity that was specifically observed in fish skin fibroblasts suggests that PS-NP uptake may have modified several cellular processes, although the analysis performed in our study does not allow us to specifically pinpoint the processes most affected. Nonetheless, an intriguing possibility is that the lysosomal pathway may be involved in the handling of PS-NPs in fish cells.

5. Conclusion

An *in vitro* approach to characterize the consequences of PS-NP uptake by human and fish skin fibroblasts was established. The results of the study indicated that cell viability, proliferation, and the cellular levels of ROS, exhibited a complex interplay that depended on factors such as dimension and concentration of PS-NP, species, and fibroblast origin (age/sex). The dynamics of cell proliferation and apoptosis influenced cell migration as determined by scratch repair. The heterogeneous response of fibroblasts induced by PS-NPs was clearly revealed by the segregation of HDF, BJ.5ta and SJD.1 fibroblasts in our PCA. Our study suggests that AP, ROS, and Caspase 2 activity are good *in vitro* indicators of PS-NP-induced cellular effects in SJD.1, BJ5TA, and HDF cells, respectively.

Supplementary data to this article can be found online at https://doi.org/10.1016/j.scitotenv.2024.169979.

CRediT authorship contribution statement

Maoxiao Peng: Writing – review & editing, Writing – original draft, Visualization, Validation, Methodology, Investigation, Formal analysis, Data curation. **Rute C. Félix:** Writing – review & editing, Writing – original draft, Visualization, Validation, Methodology, Investigation, Data curation. **Adelino V.M. Canário:** Writing – review & editing, Supervision, Resources, Project administration, Methodology, Funding acquisition. **Deborah M. Power:** Writing – review & editing, Writing – original draft, Validation, Supervision, Resources, Project administration, Methodology, Funding acquisition, Conceptualization.

Declaration of competing interest

The authors declare that they have no known competing financial interests or personal relationships that could have appeared to influence the work reported in this paper.

Data availability

No data was used for the research described in the article.

Acknowledgements

This study received Portuguese national funds from FCT - Foundation for Science and Technology through projects UIDB/04326/2020 (DOI:10.54499/UIDB/0436/2020), UIDP/04326/2020 (DOI:10.54499/UIDP/04326/2020) and LA/P/0101/2020 (DOI:10.54499/LA/P/0101/2020), and from the operational programs CRESC Algarve 2020 and COMPETE 2020 through the project EMBRC.PT ALG-01-0145-FEDER-022121. The PLASTIFISH project was financed by the Portuguese Foundation for Science and Technology (FCT) and Macao Science and Technology Development Fund (FDCT) FDCT0004/2019/AP (DOI:10.54499/MACAU/0001/2019). RCF was funded by FCT, under the "Norma Transitória" – DL57/2016/CP1361/CT0020.

References

Abe, G., Hayashi, T., Yoshida, K., Yoshida, T., Kudoh, H., Sakamoto, J., Konishi, A., Kamei, Y., Takeuchi, T., Tamura, K., Yokoyama, H., 2020. Insights regarding skin regeneration in non-amniote vertebrates: skin regeneration without scar formation and potential step-up to a higher level of regeneration. Semin. Cell Dev. Biol. 100, 109–121. https://doi.org/10.1016/j.semcdb.2019.11.014.

Anand, A., Srivastava, P.K., 2012. A molecular description of acid phosphatase. Appl. Biochem. Biotechnol. https://doi.org/10.1007/s12010-012-9694-8.

Andrady, A.L., 2011. Microplastics in the marine environment. Mar. Pollut. Bull. https://doi.org/10.1016/j.marpolbul.2011.05.030.

Banerjee, A., Billey, L.O., Shelver, W.L., 2021. Uptake and toxicity of polystyrene micro/nanoplastics in gastric cells: effects of particle size and surface functionalization. PLoS One 16. https://doi.org/10.1371/journal.pone.0260803.

Barboza, L.G.A., Lopes, C., Oliveira, P., Bessa, F., Otero, V., Henriques, B., Raimundo, J., Caetano, M., Vale, C., Guilhermino, L., 2020. Microplastics in wild fish from North East Atlantic Ocean and its potential for causing neurotoxic effects, lipid oxidative damage, and human health risks associated with ingestion exposure. Sci. Total Environ. 717 https://doi.org/10.1016/j.scitotenv.2019.134625.

Barría, C., Brandts, I., Tort, L., Oliveira, M., Teles, M., 2020. Effect of nanoplastics on fish health and performance: a review. Mar. Pollut. Bull. https://doi.org/10.1016/j.marpolbul.2019.110791.

Bobori, D.C., Dimitriadi, A., Feidantsis, K., Samiotaki, A., Fafouti, D., Sampsonidis, I., Kalogiannis, S., Kastrinaki, G., Lambropoulou, D.A., Kyzas, G.Z., Koumoundouros, G., Bikiaris, D.N., Kaloyianni, M., 2022. Differentiation in the expression of toxic effects of polyethylene-microplastics on two freshwater fish species: size matters. Sci. Total Environ. 830 https://doi.org/10.1016/j.scitotenv.2022.154603.

Boucher, J., Faure, F., Pompini, O., Plummer, Z., Wieser, O., Felippe de Alencastro, L., 2019. (Micro) plastic fluxes and stocks in Lake Geneva basin. TrAC Trends Anal. Chem. https://doi.org/10.1016/j.trac.2018.11.037.

Bouwstra, J., Pilgram, G., Gooris, G., Koerten, H., Ponec, M., 2001. New aspects of the skin barrier organization. Skin Pharmacol. Appl. Ski. Physiol. 14 https://doi.org/10.1159/000056391.

Braff, M.H., Gallo, R.L., 2006. Antimicrobial peptides: an essential component of the skin defensive barrier. Curr. Top. Microbiol. Immunol. https://doi.org/10.1007/3-540-29916-5_4.

Bull, H., Murray, P.G., Thomas, D., Fraser, A.M., Nelson, P.N., 2002. Acid phosphatases. J. Clin. Pathol. Mol. Pathol. https://doi.org/10.1136/mp.55.2.65.

Carballo, C., Firmino, J., Anjos, L., Santos, S., Power, D.M., Manchado, M., 2018. Short- and long-term effects on growth and expression patterns in response to incubation temperatures in Senegalese sole. Aquaculture. https://doi.org/10.1016/j.aquaculture.2018.05.043.

Chang, X., Fang, Y., Wang, Y., Wang, F., Shang, L., Zhong, R., 2022. Microplastic pollution in soils, plants, and animals: a review of distributions, effects and potential mechanisms. Sci. Total Environ. https://doi.org/10.1016/j.scitotenv.2022.157857.

Chen, Y., Awasthi, A.K., Wei, F., Tan, Q., Li, J., 2021. Single-use plastics: production, usage, disposal, and adverse impacts. Sci. Total Environ. https://doi.org/10.1016/j.scitotenv.2020.141772.

Cortés, C., Domenech, J., Salazar, M., Pastor, S., Marcos, R., Hernández, A., 2020. Nanoplastics as a potential environmental health factor: effects of polystyrene nanoparticles on human intestinal epithelial Caco-2 cells. Environ. Sci. Nano 7. https://doi.org/10.1039/c9en00523d.

Cózar, A., Echevarría, F., González-Gordillo, J.I., Irigoien, X., Úbeda, B., Hernández-León, S., Palma, Á.T., Navarro, S., García-de-Lomas, J., Ruiz, A., Fernández-de-Puelles, M.L., Duarte, C.M., 2014. Plastic debris in the open ocean. Proc. Natl. Acad. Sci. U. S. A. 111 https://doi.org/10.1073/pnas.1314705111.

Cózar, A., Martí, E., Duarte, C.M., García-de-Lomas, J., Van Sebille, E., Ballatore, T.J., Eguíluz, V.M., Ignacio González-Gordillo, J., Pedrotti, M.L., Echevarría, F., Troublè, R., Irigoien, X., 2017. The Arctic Ocean as a dead end for floating plastics in the North Atlantic branch of the thermohaline circulation. Sci. Adv. 3 https://doi.org/10.1126/sciadv.1600582.

de Souza Machado, A.A., Kloas, W., Zarfl, C., Hempel, S., Rillig, M.C., 2018. Microplastics as an emerging threat to terrestrial ecosystems. Glob. Chang. Biol. https://doi.org/10.1111/gcb.14020.

del Real, A.E.P., Mitrano, D.M., Castillo-Michel, H., Wazne, M., Reyes-Herrera, J., Bortel, E., Hesse, B., Villanova, J., Sarret, G., 2022. Assessing implications of nanoplastics exposure to plants with advanced nanometrology techniques. J. Hazard. Mater. 430, 128356 https://doi.org/10.1016/J.JHAZMAT.2022.128356.

Desidery, L., Lanotte, M., 2022. Polymers and plastics: Types, properties, and manufacturing, in: Plastic Waste for Sustainable Asphalt Roads. https://doi.org/10.1016/B978-0-323-85789-5.00001-0.

Dissanayake, P.D., Kim, S., Sarkar, B., Oleszczuk, P., Sang, M.K., Haque, M.N., Ahn, J.H., Bank, M.S., Ok, Y.S., 2022. Effects of microplastics on the terrestrial environment: a critical review. Environ. Res. 209 https://doi.org/10.1016/j.envres.2022.112734.

Eerkes-Medrano, D., Thompson, R.C., Aldridge, D.C., 2015. Microplastics in freshwater systems: a review of the emerging threats, identification of knowledge gaps and prioritisation of research needs. Water Res. https://doi.org/10.1016/j.watres.2015.02.012.

Elsayed Azab, A., A Adwas, Almokhtar, Ibrahim Elsayed, A.S., A Adwas, A., Elsayed, Ibrahim, Sedik, Ata, Quwaydir, F.A., 2019. Oxidative stress and antioxidant mechanisms in human body. J. Appl. Biotechnol. Bioeng. 6 https://doi.org/10.15406/jabb.2019.06.00173.

Eming, S.A., Martin, P., Tomic-canic, M., Park, H., Medicine, R., 2014. Wound repair and regeneration: mechanism, signaling and translation. Sci. Transl. Med. 6 https://doi.org/10.1126/scitranslmed.3009337.

Etienne-Manneville, S., 2004. Actin and microtubules in cell motility: which one is in control? Traffic. https://doi.org/10.1111/j.1600-0854.2004.00196.x.

Etienne-Manneville, S., 2013. Microtubules in cell migration. Annu. Rev. Cell Dev. Biol. 29, 471–499. https://doi.org/10.1146/annurev-cellbio-101011-155711.

Félix, R.C., Anjos, L., Costa, R.A., Letsiou, S., Power, D.M., 2021. Cartilage acidic protein a novel therapeutic factor to improve skin damage repair? Mar. Drugs 19. https://doi.org/10.3390/MD19100541.

Filomeni, G., De Zio, D., Cecconi, F., 2015. Oxidative stress and autophagy: the clash between damage and metabolic needs. Cell Death Differ. https://doi.org/10.1038/cdd.2014.150.

Fiorentino, I., Gualtieri, R., Barbato, V., Mollo, V., Braun, S., Angrisani, A., Turano, M., Furia, M., Netti, P.A., Guarnieri, D., Fusco, S., Talevi, R., 2015. Energy independent uptake and release of polystyrene nanoparticles in primary mammalian cell cultures. Exp. Cell Res. 330 https://doi.org/10.1016/j.yexcr.2014.09.017.

Garcin, C., Straube, A., 2019. Microtubules in cell migration. Essays Biochem. 63, 509–520. https://doi.org/10.1042/EBC20190016.

Gautam, R., Jo, J.H., Acharya, M., Maharjan, A., Lee, D.E., Pramod, P.B., Kim, C.Y., Kim, K.S., Kim, H.A., Heo, Y., 2022. Evaluation of potential toxicity of polyethylene microplastics on human derived cell lines. Sci. Total Environ. 838 https://doi.org/10.1016/j.scitotenv.2022.156089.

Guzzetti, E., Sureda, A., Tejada, S., Faggio, C., 2018. Microplastic in marine organism: environmental and toxicological effects. Environ. Toxicol. Pharmacol. 64, 164–171. https://doi.org/10.1016/J.ETAP.2018.10.009.

He, Y., Li, J., Chen, J., Miao, X., Li, G., He, Q., Xu, H., Li, H., Wei, Y., 2020. Cytotoxic effects of polystyrene nanoplastics with different surface functionalization on human HepG2 cells. Sci. Total Environ. 723 https://doi.org/10.1016/j.scitotenv.2020.138180.

Hou, J., Lei, Z., Cui, L., Hou, Y., Yang, L., An, R., Wang, Q., Li, S., Zhang, H., Zhang, L., 2021. Polystyrene microplastics lead to pyroptosis and apoptosis of ovarian granulosa cells via NLRP3/Caspase-1 signaling pathway in rats. Ecotoxicol. Environ. Saf. 212 https://doi.org/10.1016/j.ecoenv.2021.112012.

Hu, K., Yang, Y., Zuo, J., Tian, W., Wang, Y., Duan, X., Wang, S., 2022. Emerging microplastics in the environment: properties, distributions, and impacts. Chemosphere. https://doi.org/10.1016/j.chemosphere.2022.134118.

Jambeck, J.R., Geyer, R., Wilcox, C., Siegler, T.R., Perryman, M., Andrady, A., Narayan, R., Law, K.L., 2015. Plastic waste inputs from land into the ocean. Science 347. https://doi.org/10.1126/science.1260352.

Jatana, S., Callahan, L.M., Pentland, A.P., DeLouise, L.A., 2016. Impact of cosmetic lotions on nanoparticle penetration through ex vivo C57Bl/6 hairless mouse and human skin: a comparison study. Cosmetics 3. https://doi.org/10.3390/cosmetics3010006.

Jeon, S., Clavadetscher, J., Lee, D.-K., Chankeshwara, S.V., Bradley, M., Cho, W.-S., 2018. Surface charge-dependent cellular uptake of polystyrene nanoparticles. Nanomaterials 8. https://doi.org/10.3390/nano8121028.

Jeong, C.B., Won, E.J., Kang, H.M., Lee, M.C., Hwang, D.S., Hwang, U.K., Zhou, B., Souissi, S., Lee, S.J., Lee, J.S., 2016. Microplastic size-dependent toxicity, oxidative stress induction, and p-JNK and p-p38 activation in the Monogonont rotifer (Brachionus koreanus). Environ. Sci. Technol. 50 https://doi.org/10.1021/acs.est.6b01441.

Jeong, H., Kim, W., Choi, D., Heo, J., Han, U., Jung, S.Y., Park, H.H., Hong, S.T., Park, J. H., Hong, J., 2022. Potential threats of nanoplastic accumulation in human induced pluripotent stem cells. Chem. Eng. J. 427 https://doi.org/10.1016/j.cej.2021.131841.

Jiang, B., Kauffman, A.E., Li, L., McFee, W., Cai, B., Weinstein, J., Lead, J.R., Chatterjee, S., Scott, G.I., Xiao, S., 2020. Health impacts of environmental contamination of micro- and nanoplastics: a review. Environ. Health Prev. Med. https://doi.org/10.1186/s12199-020-00870-9.

Kassambara, A., Mundt, F., 2017. Factoextra: Extract and Visualize the Results of Multivariate Data Analyses [Computer Sofware, Package] (R Packag. version).

Khan, A.Q., Travers, J.B., Kemp, M.G., 2018. Roles of UVA radiation and DNA damage responses in melanoma pathogenesis. Environ. Mol. Mutagen. https://doi.org/10.1002/em.22176.

Krishnan, V., Mitragotri, S., 2020. Nanoparticles for topical drug delivery: potential for skin cancer treatment. Adv. Drug Deliv. Rev. 153, 87–108. https://doi.org/10.1016/j.addr.2020.05.011.
Krötzsch, E., Salgado, R.M., Caba, D., Lichtinger, A., Padilla, L., Di Silvio, M., 2008. 162 alkaline phosphatase activity is related to acute inflammation and collagen turnover during acute and chronic wound healing. Wound Repair Regen. 13 https://doi.org/10.1111/j.1067-1927.2005.130216bn.x.
Kumar, M., Chen, H., Sarsaiya, S., Qin, S., Liu, H., Awasthi, M.K., Kumar, S., Singh, L., Zhang, Z., Bolan, N.S., Pandey, A., Varjani, S., Taherzadeh, M.J., 2021. Current research trends on micro- and nano-plastics as an emerging threat to global environment: a review. J. Hazard. Mater. 409 https://doi.org/10.1016/j.jhazmat.2020.124967.
Lehner, R., Weder, C., Petri-Fink, A., Rothen-Rutishauser, B., 2019. Emergence of nanoplastic in the environment and possible impact on human health. Environ. Sci. Technol. 53, 1748–1765. https://doi.org/10.1021/acs.est.8b05512.
Lenz, R., Enders, K., Nielsen, T.G., 2016. Microplastic exposure studies should be environmentally realistic. Proc. Natl. Acad. Sci. U. S. A. https://doi.org/10.1073/pnas.1606615113.
Leslie, H.A., van Velzen, M.J.M., Brandsma, S.H., Vethaak, A.D., Garcia-Vallejo, J.J., Lamoree, M.H., 2022. Discovery and quantification of plastic particle pollution in human blood. Environ. Int. 163 https://doi.org/10.1016/j.envint.2022.107199.
Lesniak, A., Salvati, A., Santos-Martinez, M.J., Radomski, M.W., Dawson, K.A., Åberg, C., 2013. Nanoparticle adhesion to the cell membrane and its effect on nanoparticle uptake efficiency. J. Am. Chem. Soc. 135 https://doi.org/10.1021/ja309812z.
Letsiou, S., Félix, R.C., Cardoso, J.C.R., Anjos, L., Mestre, A.L., Gomes, H.L., Power, D.M., 2020. Cartilage acidic protein 1 promotes increased cell viability, cell proliferation and energy metabolism in primary human dermal fibroblasts. Biochimie 171–172, 72–78. https://doi.org/10.1016/j.biochi.2020.02.008.
Li, Z., Feng, C., Wu, Y., Guo, X., 2020. Impacts of nanoplastics on bivalve: fluorescence tracing of organ accumulation, oxidative stress and damage. J. Hazard. Mater. 392, 122418 https://doi.org/10.1016/j.jhazmat.2020.122418.
Li, Y., Wang, Z., Guan, B., 2022. Separation and identification of nanoplastics in tap water. Environ. Res. 204 https://doi.org/10.1016/j.envres.2021.112134.
Li, Yu, Li, Yaning, Li, J., Song, Z., Zhang, C., Guan, B., 2023. Toxicity of polystyrene nanoplastics to human embryonic kidney cells and human normal liver cells: effect of particle size and Pb2+ enrichment. Chemosphere 328, 138545. https://doi.org/10.1016/J.CHEMOSPHERE.2023.138545.
Lihua, C., Zhiyin, T., 2023. Microplastics aggravates rheumatoid arthritis by affecting the proliferation/migration/inflammation of fibroblast-like synovial cells by regulating mitochondrial homeostasis. Int. Immunopharmacol. 120 https://doi.org/10.1016/j.intimp.2023.110268.
Lin, S., Zhang, H., Wang, C., Su, X.L., Song, Y., Wu, P., Yang, Z., Wong, M.H., Cai, Z., Zheng, C., 2022. Metabolomics reveal nanoplastic-induced mitochondrial damage in human liver and lung cells. Environ. Sci. Technol. 56 https://doi.org/10.1021/acs.est.2c03980.
Lins, T.F., O'Brien, A.M., Kose, T., Rochman, C.M., Sinton, D., 2022. Toxicity of nanoplastics to zooplankton is influenced by temperature, salinity, and natural particulate matter. Environ. Sci. Nano 9. https://doi.org/10.1039/d2en00123c.
Liu, L., Xu, K., Zhang, B., Ye, Y., Zhang, Q., Jiang, W., 2021. Cellular internalization and release of polystyrene microplastics and nanoplastics. Sci. Total Environ. 779 https://doi.org/10.1016/j.scitotenv.2021.146523.
Liu, L., Liu, B., Zhang, B., Ye, Y., Jiang, W., 2022. Polystyrene micro(nano)plastics damage the organelles of RBL-2H3 cells and promote MOAP-1 to induce apoptosis. J. Hazard. Mater. 438 https://doi.org/10.1016/j.jhazmat.2022.129550.
Mendes, L.A., 2022. Microplastics effects in the terrestrial environment, in: Handbook of Microplastics in the Environment. https://doi.org/10.1007/978-3-030-39041-9_46.
Mortensen, L.J., Oberdörster, G., Pentland, A.P., DeLouise, L.A., 2008. In vivo skin penetration of quantum dot nanoparticles in the murine model: the effect of UVR. Nano Lett. 8 https://doi.org/10.1021/nl801323y.
Niethammer, P., Grabher, C., Look, A.T., Mitchison, T.J., 2009. A tissue-scale gradient of hydrogen peroxide mediates rapid wound detection in zebrafish. Nature. https://doi.org/10.1038/nature08119.
Pelegrini, K., Pereira, T.C.B., Maraschin, T.G., Teodoro, L.D.S., Basso, N.R.D.S., De Galland, G.L.B., Ligabue, R.A., Bogo, M.R., 2023. Micro- and nanoplastic toxicity: a review on size, type, source, and test-organism implications. Sci. Total Environ. https://doi.org/10.1016/j.scitotenv.2023.162954.
Peng, L., Fu, D., Qi, H., Lan, C.Q., Yu, H., Ge, C., 2020. Micro- and nano-plastics in marine environment: source, distribution and threats — a review. Sci. Total Environ. https://doi.org/10.1016/j.scitotenv.2019.134254.
Plastics Europe, 2022. Plastics-The Facts 2022 OCTOBER 2022. Plast. - Facts, 2022, p. 81.
Poma, A., Vecchiotti, G., Colafarina, S., Zarivi, O., Aloisi, M., Arrizza, L., Chichiriccò, G., Di Carlo, P., 2019. In vitro genotoxicity of polystyrene nanoparticles on the human fibroblast hs27 cell line. Nanomaterials 9. https://doi.org/10.3390/nano9091299.
Rakers, S., Gebert, M., Uppalapati, S., Meyer, W., Anderson, P., Sell, A.F., Kruse, C., Paus, R., 2010. Fish matters': the relevance of fish skin biology to investigative dermatology. Exp. Dermatol. 19 (4), 313–324. https://doi.org/10.1111/j.1600-0625.2009.01059.x.
Revelle, W., 2016. Procedures for Personality and Psychological Research, NorthwesternUniversity, Evanston, Illinois, USA. R Packag. Publ. through CRAN 1.6.12.
Richardson, R., Slanchev, K., Kraus, C., Knyphausen, P., Eming, S., Hammerschmidt, M., 2013. Adult zebrafish as a model system for cutaneous wound-healing research. J. Invest. Dermatol. 133, 1655–1665. https://doi.org/10.1038/jid.2013.16.
Rodrigues, M., Kosaric, N., Bonham, C.A., Gurtner, G.C., 2019. Wound healing: a cellular perspective. Physiol. Rev. 99 https://doi.org/10.1152/physrev.00067.2017.
Rubio, L., Barguilla, I., Domenech, J., Marcos, R., Hernández, A., 2020a. Biological effects, including oxidative stress and genotoxic damage, of polystyrene nanoparticles in different human hematopoietic cell lines. J. Hazard. Mater. 398 https://doi.org/10.1016/j.jhazmat.2020.122900.
Rubio, L., Marcos, R., Hernández, A., 2020b. Potential adverse health effects of ingested micro- and nanoplastics on humans. Lessons learned from in vivo and in vitro mammalian models. J. Toxicol. Environ. Health B Crit. Rev. 23, 51–68. https://doi.org/10.1080/10937404.2019.1700598.
Sana, S.S., Dogiparthi, L.K., Gangadhar, L., Chakravorty, A., Abhishek, N., 2020. Effects of microplastics and nanoplastics on marine environment and human health. Environ. Sci. Pollut. Res. 27 https://doi.org/10.1007/s11356-020-10573-x.
Schmidt, A., da Silva Brito, W.A., Singer, D., Mühl, M., Berner, J., Saadati, F., Wolff, C., Miebach, L., Wende, K., Bekeschus, S., 2023. Short- and long-term polystyrene nano- and microplastic exposure promotes oxidative stress and divergently affects skin cell architecture and Wnt/beta-catenin signaling. Part. Fibre Toxicol. 20 https://doi.org/10.1186/s12989-023-00513-1.
Schneider, M., Stracke, F., Hansen, S., Schaefer, U.F., 2009. Nanoparticles and their interactions with the dermal barrier. Dermatoendocrinology 1. https://doi.org/10.4161/derm.1.4.9501.
Schymanski, D., Goldbeck, C., Humpf, H.U., Fürst, P., 2018. Analysis of microplastics in water by micro-Raman spectroscopy: release of plastic particles from different packaging into mineral water. Water Res. 129 https://doi.org/10.1016/j.watres.2017.11.011.
Shekaran, A., García, A.J., 2011. Extracellular matrix-mimetic adhesive biomaterials for bone repair. J. Biomed. Mater. Res. A. https://doi.org/10.1002/jbm.a.32979.
Shen, Y., Jing, D., Zhao, Z., 2022. The effect of AKT in extracellular matrix stiffness induced osteogenic differentiation of hBMSCs. Cell. Signal. 99 https://doi.org/10.1016/j.cellsig.2022.110404.
Shi, Q., Tang, J., Liu, X., Liu, R., 2021. Ultraviolet-induced photodegradation elevated the toxicity of polystyrene nanoplastics on human lung epithelial A549 cells. Environ. Sci. Nano 8. https://doi.org/10.1039/d1en00465d.
Ter Halle, A., Jeanneau, L., Martignac, M., Jardé, E., Pedrono, B., Brach, L., Gigault, J., 2017. Nanoplastic in the North Atlantic subtropical gyre. Environ. Sci. Technol. 51 https://doi.org/10.1021/acs.est.7b03667.
Thushari, G.G.N., Senevirathna, J.D.M., 2020. Plastic pollution in the marine environment. Heliyon. https://doi.org/10.1016/j.heliyon.2020.e04709.
Volff, J.-N., 2005. Genome evolution and biodiversity in teleost fish. Heredity (Edinb.) 94, 280–294. https://doi.org/10.1038/sj.hdy.6800635.
Walker, T.R., Fequet, L., 2023. Current trends of unsustainable plastic production and micro(nano)plastic pollution. TrAC Trends Anal. Chem. https://doi.org/10.1016/j.trac.2023.116984.
Wang, T., Bai, J., Jiang, X., Nienhaus, G.U., 2012. Cellular uptake of nanoparticles by membrane penetration: a study combining confocal microscopy with FTIR spectroelectrochemistry. ACS Nano 6. https://doi.org/10.1021/nn203892h.
Wang, L., Wu, W.M., Bolan, N.S., Tsang, D.C.W., Li, Y., Qin, M., Hou, D., 2021. Environmental fate, toxicity and risk management strategies of nanoplastics in the environment: current status and future perspectives. J. Hazard. Mater. 401 https://doi.org/10.1016/j.jhazmat.2020.123415.
Wickham, H., 2012. reshape2: Flexibly Reshape Data: A Reboot of the Reshape Package (R Packag. version).
Wickham, H., 2016. Package 'ggplot2': Elegant Graphics for Data Analysis. Springer-Verlag, New York.
Wu, B., Wu, X., Liu, S., Wang, Z., Chen, L., 2019. Size-dependent effects of polystyrene microplastics on cytotoxicity and efflux pump inhibition in human Caco-2 cells. Chemosphere 221. https://doi.org/10.1016/j.chemosphere.2019.01.056.
Xu, M., Halimu, G., Zhang, Q., Song, Y., Fu, X., Li, Yongqiang, Li, Yansheng, Zhang, H., 2019. Internalization and toxicity: a preliminary study of effects of nanoplastic particles on human lung epithelial cell. Sci. Total Environ. 694 https://doi.org/10.1016/j.scitotenv.2019.133794.
Xu, X., Feng, Y., Han, C., Yao, Z., Liu, Y., Luo, C., Sheng, J., 2023. Autophagic response of intestinal epithelial cells exposed to polystyrene nanoplastics. Environ. Toxicol. 38, 205–215. https://doi.org/10.1002/tox.23678.
Zeng, L., Gowda, B.H.J., Ahmed, M.G., Abourehab, M.A.S., Chen, Z.-S., Zhang, C., Li, J., Kesharwani, P., 2023. Advancements in nanoparticle-based treatment approaches for skin cancer therapy. Mol. Cancer 22, 10. https://doi.org/10.1186/s12943-022-01708-4.
Zhang, D., Liu, H. bin, Hu, W. li, Qin, X. hui, Ma, X. wang, Yan, C. rong, Wang, H. yuan, 2016. The status and distribution characteristics of residual mulching film in Xinjiang, China. J. Integr. Agric. 15 https://doi.org/10.1016/S2095-3119(15)61240-0.
Zhou, X.X., Hao, L.T., Wang, H.Y.Z., Li, Y.J., Liu, J.F., 2019. Cloud-point extraction combined with thermal degradation for nanoplastic analysis using pyrolysis gas chromatography-mass spectrometry. Anal. Chem. 91 https://doi.org/10.1021/acs.analchem.8b04729.
Zhou, X.X., He, S., Gao, Y., Li, Z.C., Chi, H.Y., Li, C.J., Wang, D.J., Yan, B., 2021. Protein corona-mediated extraction for quantitative analysis of nanoplastics in environmental waters by pyrolysis gas chromatography/mass spectrometry. Anal. Chem. 93 https://doi.org/10.1021/acs.analchem.1c00156.